Noise Performance of Erbium-Doped Fiber Amplifiers With Forward and Reverse Pumping

by
Jessica Sinyin Tan

Submitted to the Department of Electrical Engineering and Computer Science
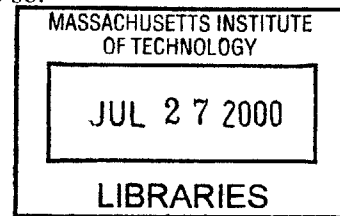*Massachusetts Institute of Technology*

In Partial Fulfillment of the Requirements for the Degrees of
Bachelor of Science in Electrical Engineering
and Master of Engineering in Electrical Engineering and Computer Science

May 11, 2000

[June 2000]

The author hereby grants to M.I.T. permission to reproduce and distribute publicly **ENG**
paper and electronic copies of this thesis and grant others the right to do so.

Author_____

Jessica Sinyin Tan
Department of Electrical Engineering and Computer Science
May 11, 2000

Certified by_____

Professor Hermann A. Haus
Thesis Supervisor

Accepted by_____

Professor Arthur C. Smith
Chairman, Department Committee on Graduate Theses

Noise Performance of Erbium-Doped Fiber Amplifiers With Forward and Reverse Pumping

by
Jessica Sinyin Tan

Submitted to the Department of Electrical Engineering and Computer Science
Massachusetts Institute of Technology

In Partial Fulfillment of the Requirements for the Degrees of
Bachelor of Science in Electrical Engineering
and Master of Engineering in Electrical Engineering and Computer Science

May 11, 2000

Technical Abstract

The noise performance of an erbium-doped fiber amplifier (EDFA) is characterized by modeling optical amplifiers as four-level or three-level systems. The gain and noise performance are then examined under forward and reverse pumping. It is found that a four-level system displays symmetrical behavior under forward and reverse pumping, while a three-level gives a better noise performance with forward pumping at the expense of gain. Analytical predictions from numerical simulations based on these models are then compared with EDFA experimental results. The concept of noise measure is also reinforced and applied in this paper.

Thesis Supervisor: Professor H. A. Haus
Title: Institute Professor, MIT Research Laboratory of Electronics (Optics Group)

Table of Contents

B. The Three-level Medium

V. Simulation Results & Analysis

A. Verifying the Four-level Model

B. Verifying the Three-level Model

C. 3-Level EDFA Experimental Setup

D. Experiment 1: Verifying the Description of the Model

E. Experiment 2: Comparing Between 980 nm and 1480 nm Pumping

VI. Conclusions

VII. Bibliography

I. Acknowledgements

I would like to thank my thesis supervisor, Professor Haus, for his inspiring guidance and invaluable discussions. Secondly, I would also like to extend my thanks to Charles X. Yu, PhD candidate for EECS, MIT, and Luc Boivin, Bell Laboratories, Lucent Technologies, for making the two experiments possible in this thesis and also for their patience and help in analyzing the experimental data. I am also pleased to have worked with Matthew Grein and Yijiang Chen, both of whom had motivated my interest in this area of topic. Finally, I would like to thank my family, especially my sister, Xinyuan Tan, and my boyfriend, Dawen Choy, who have given me great support in completing this thesis.

II. Introduction

A. *History of Optical Amplifiers*

Optical communications is developed for its superior performance in bandwidth, speed and reliability. However, its potential could not be fully harnessed in traditional optical systems because it was limited by the switching speed of electronic circuits. Although optical fibers could potentially offer a bandwidth of 45 THz between 1.3 and 1.5 μm, the bottleneck in long-distance optical communications was in the electronic repeaters that had to be placed ~ 70 km apart in order to prevent signal degradation due to attenuation and loss in fiber transmission. These electronic repeaters were in essence photodiodes and laser diodes that converted optical signals into currents and back again after regenerating the signal electronically. Since these semiconductor devices were physically limited to 10 GHz switching speeds, so were the repeatered optical transmission systems.

The exciting breakthrough was in the advent of erbium-doped fiber amplifiers (EDFAs). It was discovered that optical fibers, when doped with the rare earth erbium and excited by low powers of light, display gain characteristics around the wavelength of 1.5 μm. Furthermore, Er-doped fibers have many other desirable properties of an amplifier; namely polarization insensitivity, temperature stability and immunity to inter-channel crosstalk [1]. This finding led to the use of Er-doped fibers as optical amplifiers, replacing the need for electronic repeaters in long-distance communications systems, thus eliminating the bottleneck. Since then, commercial

systems with EDFAs have been developed, the transoceanic cables across the Atlantic and the

Pacific being one example. Data rates as high as 10 GHz have also been realized.

B. Challenges in the Industry & Motivation for Discussion

In recent years, as the need for greater capacity-carrying cables continues to scale

exponentially with the need for information and networking, there has been search for new

improvements to increase the bandwidth of the fibers. For example, commercial EDFAs are now

equipped with dispersion-compensating fibers (DCF) so that inter-symbol interference due to

dispersion in the transmitting fibers is suppressed. This is especially important in *Wavelength*

Division Multiplexing (WDM) systems because channels can thus be more closely spaced in

frequency without fear of inter-channel crosstalk. The downside of this approach is that DCFs are

rather lossy so the noise figure of the EDFA module increases and the signal-to-noise ratio (SNR)

deteriorates.

Another proposition that is currently being researched is to increase the intensity of the

signals so that the same amount of information can be sent with a shorter pulse. In this way, the

data rate can be increased while maintaining a certain SNR. However, as intensity of light

increases in the fiber, nonlinear effects of the fiber become dominant and other means are needed

to correct for the nonlinearities. Like DCFs, these corrections tend to deteriorate the gain and

SNR as well.

It seems unavoidable that any improvements in bandwidth are at the expense of gain and SNR. The challenge in the industry is thus to improve bandwidth without compromising the gain and SNR significantly. This provides the impetus for the discussion in this paper. If the noise performance of the EDFAs can be further improved without too much gain deterioration, improvements can be made elsewhere in the transmission system to increase the bandwidth without signal degradation. EDFAs can therefore act as more efficient amplifiers without introducing too much noise on their own[1].

The aim of this thesis is to characterize and compare the noise performance of an optical amplifier under forward and reverse pumping, in particular focusing on the EDFA. In order to gain insight into the phenomena determining the gain and noise characteristics, EDFAs are first modeled mathematically as optical amplifiers. The analytical predictions of these models are then verified with computer simulations and experimental results.

III. Fundamentals of Optical Amplifiers & EDFAs

A. Working Principle of an Optical Amplifier

Figure 1 shows a schematic diagram of an optical amplifier. In general there is a ground state level. A separate light source, referred to as the pump, will first excite the erbium atoms in the ground state into a higher energy level. These excited atoms then quickly relax into the metastable level where they remain for a relatively long period of time. It is crucial for optical amplifiers to maintain an abundance of atoms at the metastable level, a phenomenon here forth referred to as population inversion.

For the three-level system, these atoms will remain there until an input signal of the exact energy as the energy gap between the metastable and the ground state level passes through the medium, which stimulates the atoms in the metastable level to emit a photon of the exact frequency as the signal. This process of amplifying the signal is known as *stimulated emission*. The emitted photons emitted at the same frequency as the signal.
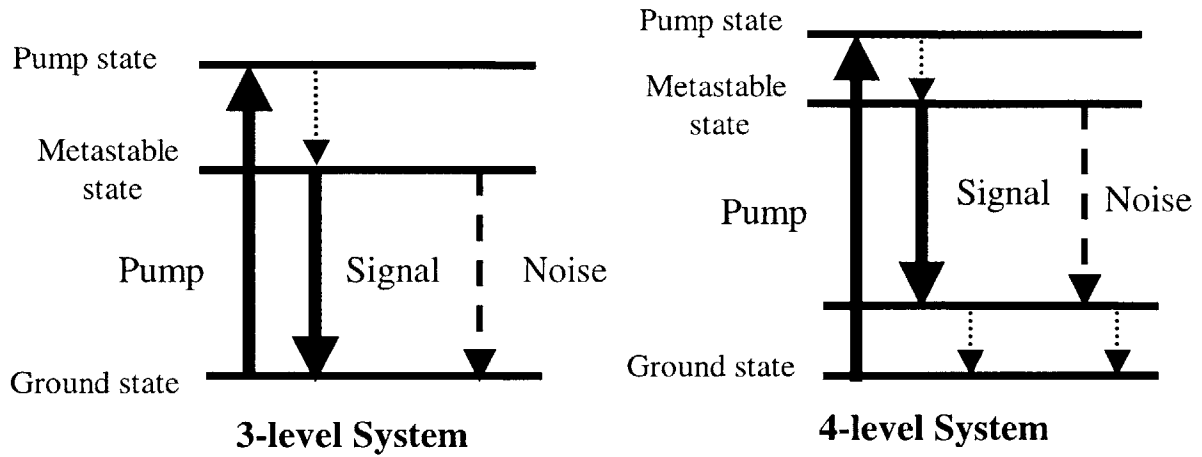
Figure 1: Schematic diagrams of an optical amplifier

Amplifier noise occurs when the atoms in the metastable level spontaneously relax to the ground state without the stimulation of the signal. *Spontaneous emission* occurs at the same frequency as the signal and is therefore amplified as well, constituting the *Amplified Spontaneous Emission* (ASE) at the output of the amplifier.

The four-level system is essentially the same as the three-level system except that the atoms at the metastable level first relax into an unstable, intermediate level before quickly falling into the ground level.

B. Why an Erbium-Doped Fiber Amplifier?

Rare earth-doped insulators have long been shown to emit or absorb an energy spectrum composed of a series of sharp narrow lines. This phenomenon was first observed in 1900s by J. Becquerel and later explained by Judd and Ofelt to be a consequence of their contracted 4f shell

atomic structure. Normally atoms in semiconductor or metal give up electrons to the solid as a

whole but for a rare earth-doped insulator, the wave function is very localized thus producing an

energy spectrum with sharp lines. This typically results in a huge energy gap in the energy level

structure. Erbium[2]-doped glass fibers are particularly desirable optical amplifiers precisely because

of its huge energy gap, and consequently its long lifetime[3] (~ 10 ms for Er-doped silica glass) and

mostly radiative relaxation of the metastable $^4I_{13/2}$ level. Therefore, a high level of population

inversion can be achieved in Er-doped glass providing a good lasing medium for an optical

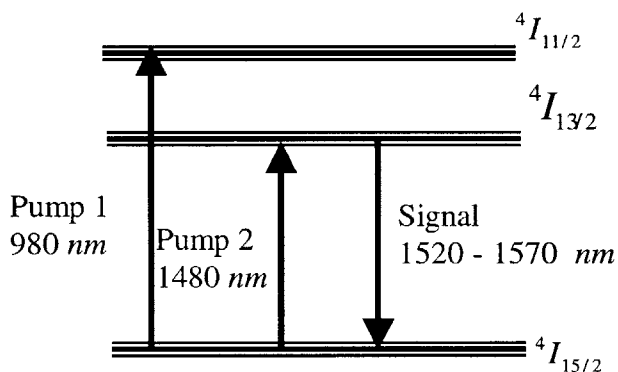amplifier. Figure 2 depicts the energy level structure of erbium.

Figure 2: Three-Level energy level structure of EDFA [3]

Moreover because the higher energy levels have mostly non-radiative relaxations, atoms

are less likely to be excited to these higher levels from the metastable level (termed *Excited State*

Absorption or ESA), which reduces the level of population inversion. In fact, when pumped at

980 nm, Er-doped fibers are almost ESA-free [2]. Maintaining a high level of population

inversion, stimulated emission occurs more readily in EDFAs. There is also less ASE that

deteriorates the amplifier noise performance.

Another reason for the popularity of EDFAs is the fact that they can be pumped easily and

11

effectively with readily available, low-powered semiconductor lasers. This is because erbium-doped fibers have a high absorption cross-section[4] and with the light being confined in fiber cores of very small dimensions, light intensities reached are very high[5]. This allows population inversion to be achieved with relatively small pump powers[6], as that provided by semiconductor diode lasers.

C. Figures of Merit of Optical Amplifiers

There are two figures of merit commonly used to characterize the performance of an optical amplifier, namely gain G and noise measure M. They are defined as

$$G = \frac{\text{Output Signal Power}}{\text{Input Signal Power}} \tag{1}$$

$$M \equiv \frac{F-1}{1-\frac{1}{G}} = \frac{\text{Output ASE photon number}}{G-1} = \frac{<n_{ASE}>}{G-1} \tag{2}$$

Therefore

$$F = 1 + \frac{<n_{ASE}>}{G} \tag{3}$$

The reason for adopting F and M is that extensive work on amplifier noise performance optimization has used this definition [8-13]. In general, the lower the noise measure and noise figure, the better the corresponding noise performance of the amplifier.

12

A longer amplifier produces more gain since there is a longer lasing medium, but does so at the expense of noise performance since a longer amplifier also implies the population inversion deteriorates more as the pump depletes.[7] An amplifier with a higher pump power usually means a higher level of population inversion in the lasing medium and therefore more gain and higher saturation output power. Better population inversion also tends to lead to better noise performance provided the amplifier is not saturated. [1-5][8]

The focus of this paper is to examine the gain and noise measure of these amplifiers under different signal input powers, and under forward and reverse pumping conditions. The results of this analysis are deferred to later sections.

IV. Analytical Models & Simulation Results[9]

Analytical models of physical systems are useful in gaining insight into the phenomena determining system characteristics. Hence, theoretical models describing optical amplifiers are developed in this section. A simplified four-level system is discussed first followed by a three-level system. For each model, the signal, noise and pump distributions are then be evaluated. It is found that for a four-level system, even if gain saturation is included, the gain, signal, noise and noise figure can be evaluated analytically; this result is stunning because no one else in the industry has solved these equations before! Another surprising result is that the amplifier displays symmetrical gain and noise measure behavior under forward and reverse pump, which is in direct contradiction to the behavior of most practical amplifiers observed. The reason for this discrepancy is that these practical amplifiers are three-level systems which display a bias towards forward pumped amplifiers as discussed in the later part of this section. It was not until recently, when a group of scientists from Bell Laboratories reported symmetrical behavior for an erbium-ytterbium-codoped amplifier[10]. This experimental work supports my theoretical model for four-level systems because the Er-Yb-codoped amplifier is a four-level system.

A. The Simplified Four-level Medium

1. The Gain Medium

The schematic representation of a four-level system is depicted earlier in figure 1. An

efficient pump is assumed whereby the noise is mostly contributed by spontaneous emissions as indicated in the figure. As explained earlier in the figure, for laser action to occur within the medium, population inversion must be ensured in the medium. Inversion occurs when there are more atoms in the higher energy metastable level than the lower energy intermediate transition. The transitions from the excited pump level to the metastable level, and from the intermediate level to the ground level (both denoted by dotted arrows) are non-radiative for rare earth-doped fiber, so that no photons are emitted in these transitions. These non-radiative transitions are also fast so that a simplified two-level system is essentially obtained.

Although the input signal level may be small and close to the noise level, the amplifier can still potentially saturate because of a typically long relaxation time in the metastable level for most rare earth-doped fibers, especially the EDFA. The photon number per unit length of the signal and noise in a bit-interval is S_f for the forward traveling wave of the noise, S_b for the backward traveling wave. The net photon number is thus defined by

$$S_+ \equiv S_f + S_b \tag{4}$$

In a simplified four-level system, the rate equations can be simplified to two equations describing the main transition between the metastable level (here forth referred to as the upper level) and the intermediate level (or lower level). The population densities per unit length of these two levels are represented by N_u and N_l respectively.

$$\frac{dN_u}{dt} = -\sigma_u N_u - \sigma_s (N_u - N_l)S_+ + \beta S_p \tag{5}$$

15

$$\frac{dN_l}{dt} = -\sigma_l N_l + \sigma_s (N_u - N_l) S_+ \tag{6}$$

σ_u and σ_l are the emission and absorption cross-sections for the upper and lower level

respectively (in s^{-1}) while σ_s is the gain cross-section for the stimulated emission. Cross-sections

quantify the ability of an ion to absorb and emit for that transition level, and are related to the

Einstein A and B coefficients. S_p is the photon number of the pump in a bit interval and β is the

coefficient of the rate of decay of the pump along the length of the amplifier.

At steady state, $\dfrac{dN_u}{dt} = \dfrac{dN_l}{dt} = 0$, therefore the population difference per unit length

between the upper and lower levels is

$$N_u - N_l = \frac{\dfrac{\beta}{\sigma_u} S_p}{1 + \sigma_s (\dfrac{1}{\sigma_u} + \dfrac{1}{\sigma_l}) S_+} \tag{7}$$

Intuitively, in the absence of amplifier radiation or noise, the population inversion is largest when

the pump is strong and the upper level lifetime $\dfrac{1}{\sigma_u}$ is long so that there is not much decay of

atoms from the upper level. The inversion parameter χ is a measure of the strength of the

population inversion and is defined as

$$\chi \equiv \frac{N_u}{N_u - N_l} = 1 + \frac{\sigma_s}{\sigma_l} S_+ \qquad (8)$$

In contrast to a three-level system (discussed later in this section), the population inversion in a four-level system is always positive; intuitively, this is because the lower level is not the ground state level (but an intermediate unstable level) hence photon conservation need not hold between N_u and N_l so the medium can be perfectly inverted. Even in the case when the pump power is zero, the medium becomes merely transparent and the signal suffers no attenuation. This is in contrast to a three-level system where there is a pump threshold below which the medium then acts as a strong absorber instead of an amplifier.

The temporal rate of photon production at any point along the amplifier is

$$\sigma_s (N_u - N_l) S_{\pm} \qquad (9)$$

which can then be converted into a spatial rate (in units of inverse length) by division of the group velocity v_g. The gain coefficient (in units of inverse length) is then evaluated as

$$\alpha \equiv \frac{\sigma_s}{v_g}(N_u - N_l) = \frac{\dfrac{\beta}{\sigma_u}\dfrac{\sigma_s}{v_g}S_p}{1 + \sigma_s(\dfrac{1}{\sigma_u} + \dfrac{1}{\sigma_l})S_+} \qquad (10)$$

α is thus a decreasing function of S_+ indicating that the gain of the amplifier does saturate with both signal and noise.

2. The Signal and Noise Evolution

Noise is generated by spontaneous emission in the amplifier and can amplify in two directions, forward and backward. It is intuitive to imagine them as two separate propagating waves of noise generated by amplifier: S_{nf} growing from zero at the beginning of the amplifier, and S_{nb} growing from zero at the end of the amplifier. The equations for the evolution of the noise in the forward and backward traveling waves along the length of the amplifier z are

$$\frac{dS_{nf}}{dz} = \alpha S_{nf} + g\alpha\chi \tag{11}$$

$$\frac{dS_{nb}}{dz} = -\alpha S_{nf} - g\alpha\chi \tag{12}$$

g represents the degeneracy factor; $g = 1$ if the noise bandwidth is equal to the signal bandwidth, and a polarizer is used to pass only the noise in the same polarization as the signal. If no polarizer is used while the signal and noise bandwidths are identical, then $g = 2$. On the other hand, if the noise is passed through a filter of bandwidth B_f while the signal bandwidth is B_s, then $g = \dfrac{2B_f}{B_s}$ provided no polarizer is used.

The equation for signal growth is

$$\frac{dS_s}{dz} = \alpha S_s \tag{13}$$

Note that both the signal S_s and forward noise S_{nf} grow in the forward direction, so the output signal at the end of the amplifier is always accompanied by the amplified forward noise, referred to as the forward ASE.

Equations (11) and (13) can be added to obtain an equation for the growth of the sum of the signal and noise photon number propagating in the forward direction, $S_{nf} + S_s = S_f$,

$$\frac{dS_f}{dz} = \alpha S_f + g\alpha\chi \tag{14}$$

which is identical in form with that for the forward propagating noise alone. The presence of the signal is introduced simply by appropriate boundary conditions. For symmetry, backward propagating noise can be replaced by $S_b = S_{nb}$ so that equation (12) can be rewritten as

$$\frac{dS_b}{dz} = -\alpha S_b - g\alpha\chi \tag{15}$$

19

For mathematical convenience, these equations can be further simplified if they are

expressed in terms of the local photon sum $S_+ = S_f + S_b$ and by necessity, its counterpart

$S_- = S_f - S_b$ thus transforming the equations (14) and (15) to

$$\frac{dS_+}{dz} = \alpha S_-$$ (16)

$$\frac{dS_-}{dz} = \alpha[(1 + 2g\frac{\sigma_s}{\sigma_t})S_+ + 2g]$$ (17)

It is convenient to introduce a normalized variable defined by $dx = \alpha\ dz$ since then the

equations become particularly simple:

$$\frac{dS_+}{dx} = S_-$$ (18)

$$\frac{dS_-}{dx} = (1 + 2g\frac{\sigma_s}{\sigma_t})S_+ + 2g$$ (19)

The solutions of these two equations are

$$S_- = A\sinh(\mu x)$$ (20)

20

$$S_+ = \frac{A}{\mu}\cosh(\mu x) - 2g \qquad (21)$$

where A is a constant of integration and $\mu^2 = 1 + 2g\frac{\sigma_s}{\sigma_l}$. The forward and backward propagating

photon numbers are

$$S_f = \frac{1}{2}(S_+ + S_-) = \frac{1}{2}[\frac{A}{\mu}\cosh(\mu x) + A\sinh(\mu x)] - g \qquad (22)$$

$$S_b = \frac{1}{2}(S_+ - S_-) = \frac{1}{2}[\frac{A}{\mu}\cosh(\mu x) - A\sinh(\mu x)] - g \qquad (23)$$

which are both anti-symmetric and mirror images of each other about $x = 0$. (Note that for

forward and reverse pumping, S_f and S_b are also flipped about $x=0$.) S_f and S_b go to zero at x_0,

given by

$$\mu \mid x_0 \mid = \ln\{\frac{1}{\frac{2g}{A(1+\mu)} + \sqrt{[\frac{2g}{A(1+\mu)}]^2 + \frac{\mu-1}{\mu+1}}}\} = \ln[H(A)] \qquad (24)$$

Because the forward and backward noise start growing from zero at the beginning and end of the

amplifier respectively, $\pm x_0$ denotes the beginning and the end of the amplifier, provided signal is

much smaller than the noise.

Figure 3 shows the plots of S_f and S_b. It is remarkable that the evolution of the signal and noise in the forward direction and noise in the backward direction are symmetrical for forward and reverse pump.
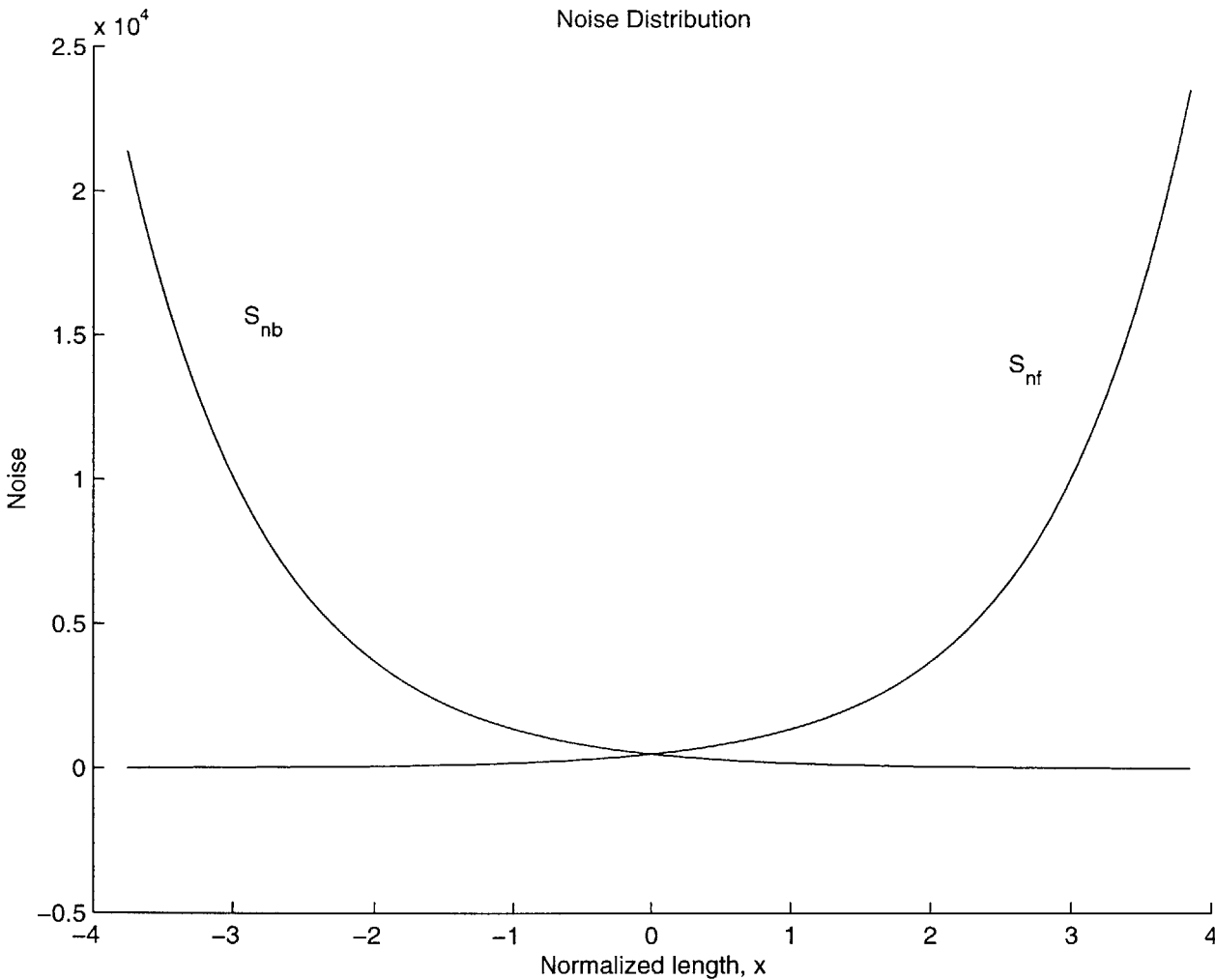

Figure 3: Noise distribution under negligible signal saturation

Gain = 19.3 dB, M = 24.4 dB; g = 1, μ = 1.001

3. Gain and Noise Measure

The gain in power of an optical amplifier is defined as

$$G = \exp\left(\int_0^L \alpha dz\right) = \exp(2x_0) = \frac{2H(A)}{\mu} \tag{25}$$

for an amplifier with negligible signal saturation where L is the length of the amplifier and the amplifier extends from $-x_0$ to $+x_0$.

As explained earlier in equation (2), the noise measure M is used to measure noise performance of optical amplifiers in this paper. From equation (3),

$$F_{ASE} - 1 = \frac{ASE_{out}}{G} = \frac{S_{nf}(x_0)}{\exp(2x_0)} \tag{26}$$

Hence using equation (4)

$$M = \frac{S_{nf}(x_0)}{g(G-1)} \tag{27}$$

4. The Evolution of the Pump

The pump loses photons at the rate of βS_p from the upper level. Similar to the treatment

of the gain coefficient, the coefficient of the temporal rate of loss β is converted into a spatial rate

by division of the group velocity v_g. Thus the equation of the pump is described as

$$\frac{dS_p}{dz} = \mp \frac{\beta}{v_g} S_p \qquad (28)$$

or in terms of the normalized variable x

$$\frac{dS_p}{dz} = \mp \frac{\beta}{\alpha v_g} S_p \qquad (29)$$

where $\mp$ holds for forward and reverse pumping respectively. Introducing the expression for the

gain coefficient, equation (10),

$$\frac{dS_p}{dx} = \mp \frac{\sigma_u}{\sigma_s} [1 + \sigma_s (\frac{1}{\sigma_u} + \frac{1}{\sigma_l}) S_+] \qquad (30)$$

Surprisingly, the right hand side of this equation does not involve the pump but only the sum of

the forward and backward propagating signal and noise, such that the rate of decay of the pump

along the normalized x does not vary with the pump level. With S_+ given by equation (21),

integrating equation (30) gives the evolution of the pump along the normalized length x

24

$$S_p = S_p(x=0) \mp \{[\frac{\sigma_u}{\sigma_s} - 2g(1+\frac{\sigma_u}{\sigma_l})]x + \frac{A}{\mu^2}(1+\frac{\sigma_u}{\sigma_l})\sinh(\mu x)\} \qquad (31)$$

where the $\mp$ signs refer to forward and reverse pumping respectively (such that the pump evolution of forward and reverse pumping are images of each other around $x=0$). Another difference between the forward and reverse pump evolution is the boundary condition at $x=0$.

On the other hand, the pump evolution along the length of the amplifier z is given by the solution of equation (28)

$$S_{p,out} = S_{p,in}e^{-\beta L} \qquad (32)$$

from which the length of the amplifier L can be obtained

$$\beta L = \ln[\frac{S_{p,in}}{S_{p,out}}] \qquad (33)$$

Figure 4 illustrates the forward pump distribution along the normalized length of the amplifier, starting from $-x_0$ to $+x_0$. Reverse pumping can be illustrated by flipping the x-axis.
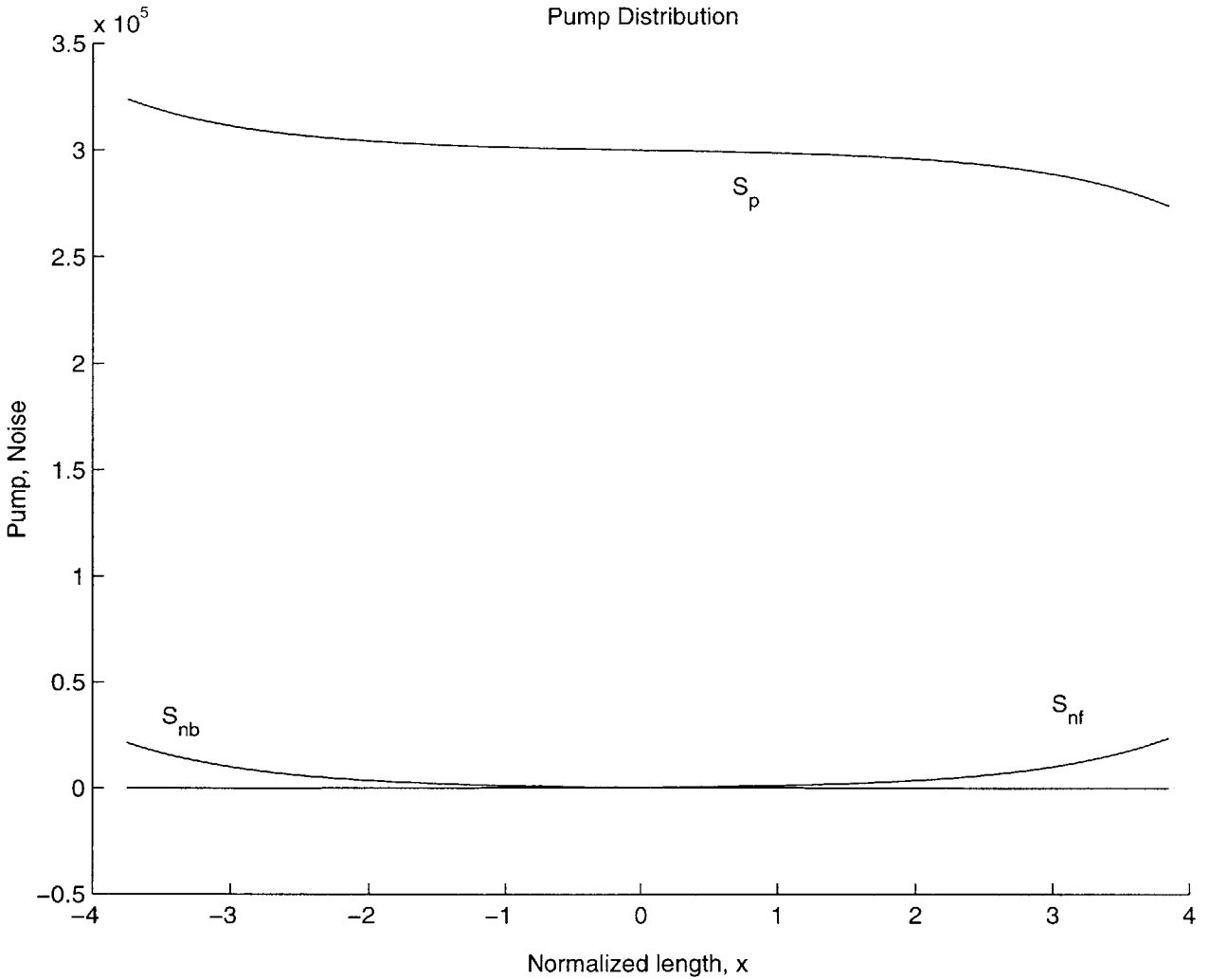
Figure 4: Pump distribution under pure noise saturation

Gain = 19.3 dB, M = 24.4 dB; Sp(x=0) = 300000, g = 1, μ = 1.001

5. Signal Saturation

Thus far, the signal has been assumed to be much smaller than the noise. Such an analysis

would be applicable in the case of a single signal channel in the presence of many unexcited

channels carrying just noise. However, with high-bandwidth demand today, the more likely

scenario is when all channels carry signal and the signal level is much greater than the noise level.

This case can be analyzed by a simple extension of the case with noise saturation only. In figure 3, instead of starting the amplifier at $-x_0$, a new reference plane can be chosen at $-x_0 + \Delta x_0$ (as shown in figure 5) for forward pumping so that the input signal of the amplifier is of the magnitude

$$S_s = \frac{1}{2}[\frac{A}{\mu}\cosh\mu(-x_0 + \Delta x_0) + A\sinh\mu(-x_0 + \Delta x_0)] - g \qquad (34)$$

In the case of reverse pumping, the new reference plane with the same input signal would be at $x_0 - \Delta x_0$ (equivalent to forward pumping case flipped across $x=0$).

Equation (34) can be used to evaluate Δx_0 for a given input signal (same for reverse pumping). As shown in figure 5, because the pump power distributions are different for the forward and reverse pumped amplifiers, the lengths are also different as suggested by equation (33). The gain can also be slightly modified from equation (25) to

$$G = \exp(|x_{out} - x_{in}|) \qquad (35)$$

where x_{in}, x_{out} represents the beginning and the end of the amplifier respectively.
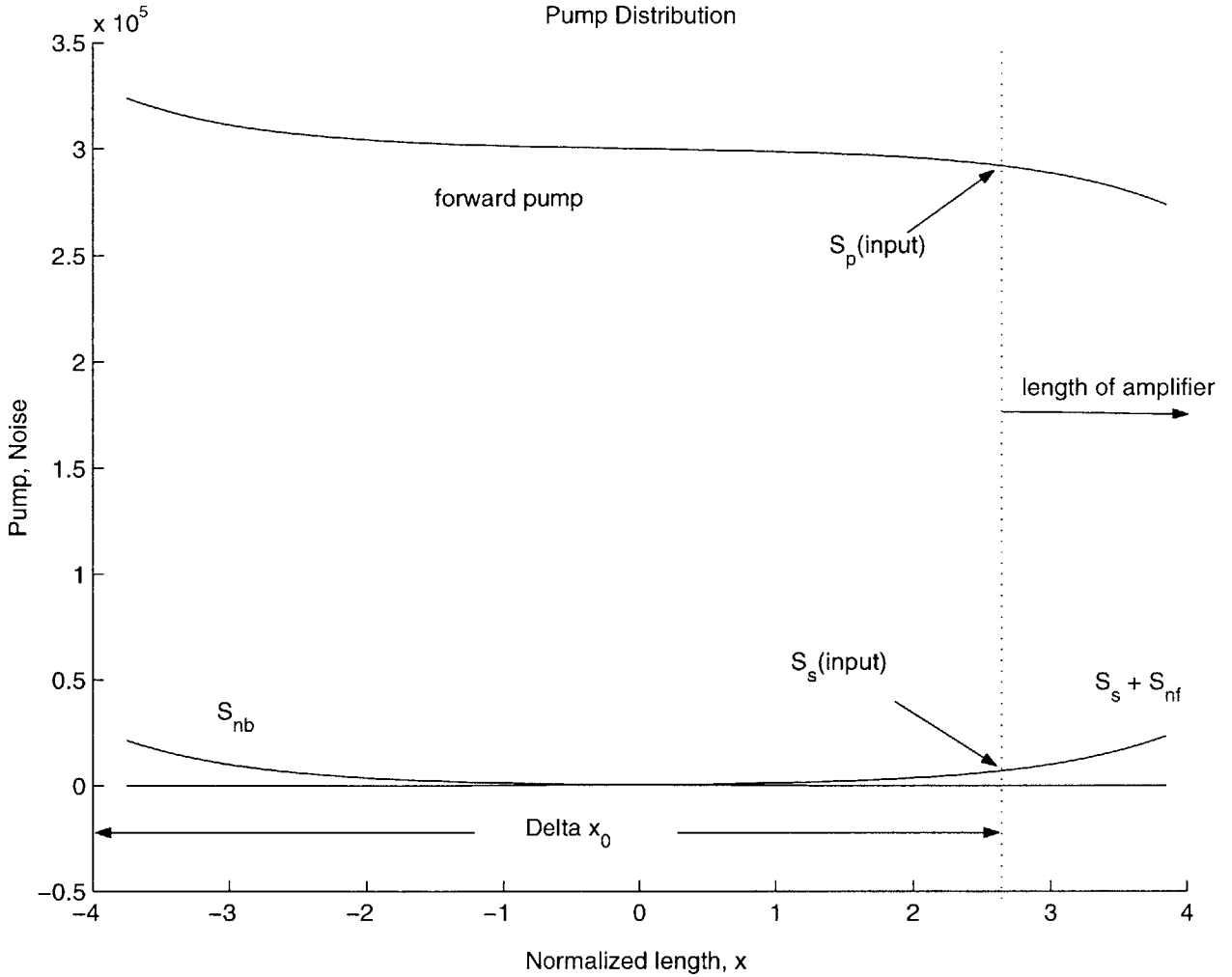
Figure 5: Signal and noise saturation (forward pump)

Gain = 19.3 dB, M = 24.4 dB; Sp(x=0) = 300000, g = 1, μ = 1.001

6. Comparison Between a Forward and Reverse Pumped Amplifier

To compare the gain and noise performance of a forward and reverse pumped amplifier, the length of the amplifiers should be adjusted to be the same. This can be achieved by a different choice of the pump parameter $S_p(0)$ so that the ratios of (input pump)/(output pump) are the same according to Equation (33). Explicitly, the input and output pump levels for both forward

and reverse pumping are

Forward Pumping: ($x_{in} = -x_0 + \Delta x_0$, $x_{out} = x_0$)

$$S_{p,in}^{forw} = S_p^{forw}(0) - \{[\frac{\sigma_u}{\sigma_s} - 2g(1 + \frac{\sigma_u}{\sigma_l})](-x_0 + \Delta x_0) + \frac{A}{\mu^2}(1 + \frac{\sigma_u}{\sigma_l})\sinh\mu(-x_0 + \Delta x_0)\} \quad (36)$$

$$S_{p,out}^{forw} = S_p^{forw}(0) - \{[\frac{\sigma_u}{\sigma_s} - 2g(1 + \frac{\sigma_u}{\sigma_l})]x_0 + \frac{A}{\mu^2}(1 + \frac{\sigma_u}{\sigma_l})\sinh(\mu x_0)\} \quad (37)$$

Reverse Pumping: ($x_{in} = x_0 - \Delta x_0$, $x_{out} = -x_0$)

$$S_{p,in}^{back} = S_p^{back}(0) - \{[\frac{\sigma_u}{\sigma_s} - 2g(1 + \frac{\sigma_u}{\sigma_l})](-x_0) + \frac{A}{\mu^2}(1 + \frac{\sigma_u}{\sigma_l})\sinh\mu(-x_0)\} \quad (38)$$

$$S_{p,out}^{back} = S_p^{back}(0) - \{[\frac{\sigma_u}{\sigma_s} - 2g(1 + \frac{\sigma_u}{\sigma_l})](x_0 - \Delta x_0) + \frac{A}{\mu^2}(1 + \frac{\sigma_u}{\sigma_l})\sinh\mu(x_0 - \Delta x_0)\} \quad (39)$$

and the length of the two amplifiers is made the same by setting

$$\frac{S_{p,in}^{forw}(-x_0 + \Delta x_0)}{S_{p,out}^{forw}(x_0)} = \frac{S_{p,in}^{back}(-x_0)}{S_{p,out}^{back}(x_0 - \Delta x_0)} \quad (40)$$

Because the pump distribution is an anti-symmetric function of x from equation (31), $S_p^{forw}(0)$ can

be raised by exactly the original difference in input pump powers $(S_{p,in}^{back} - S_{p,in}^{forw})$ to satisfy

equation (40). Figure 6 thus shows two amplifiers of the same length, input pump power, and

signal and noise evolution under forward and reverse pumping. The performance parameters of

the simulations are also summarized in Table 1. Equations (35) and (37) predict the same gain

$G = \exp(2x_0 - \Delta x_0)$ and noise measure for these two amplifiers. This analysis concludes that for a

four-level amplifying medium, the direction of pump does not affect the gain and noise

performance. The conventional wisdom in industry that forward pumped amplifiers give better

noise performance at the expense of gain does not hold for a four-level medium such as Er-Yb-

codoped fiber amplifiers and as mentioned before, this result has also been proven by experimental
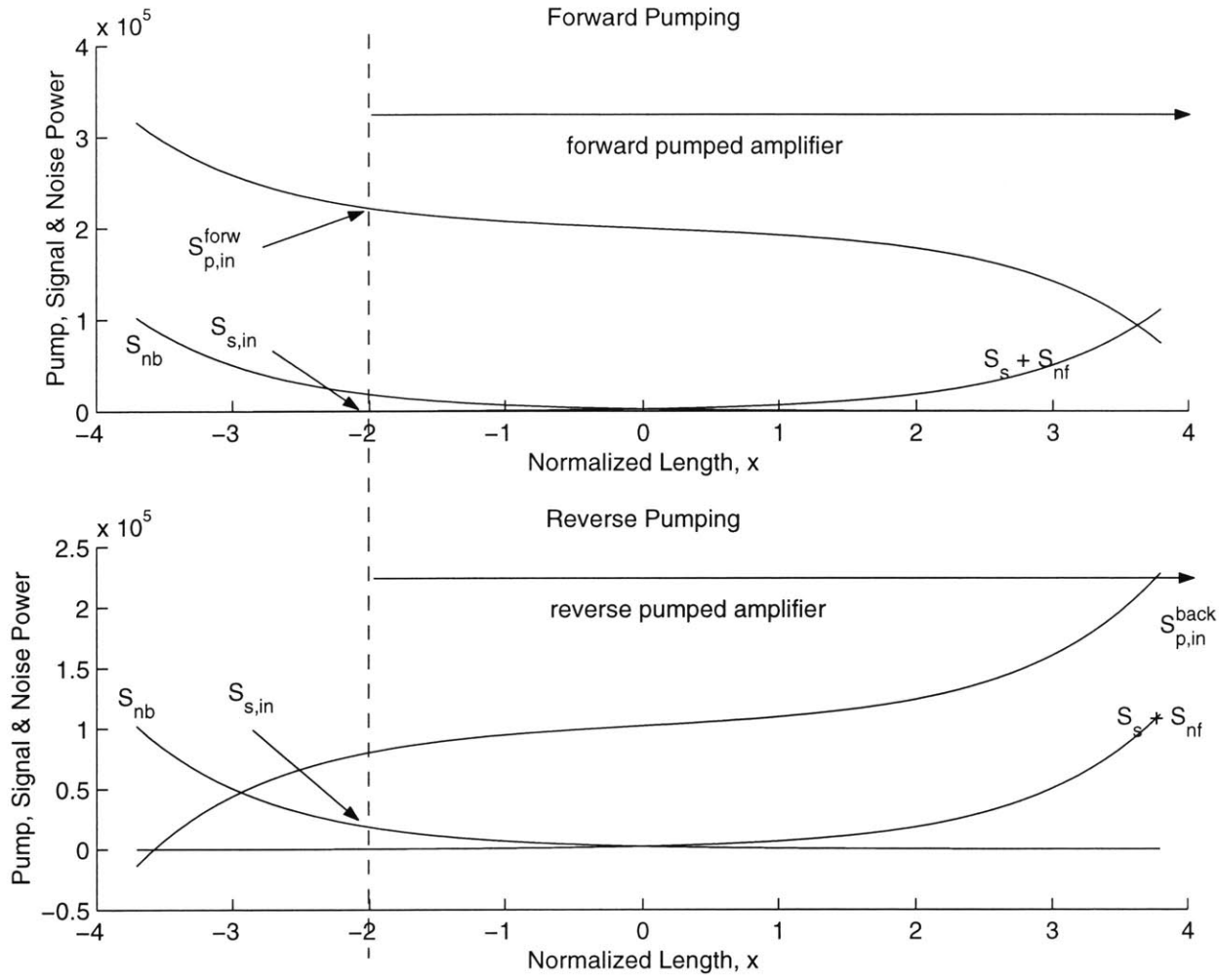
work presented at a recent conference[11].

Figure 6: Comparison between forward and reverse pumping

	G (dB)	M (dB)	Length in z, L
Forward Pumping	25.2	3.28	≈ 54.8
Reverse Pumping	25.2	3.28	≈ 52.3

Table 1: Simulation results for simplified four-level amplifier

$g = 10; \ \mu = 1.001$

B. The Three-Level Medium

1. The Gain Medium

The energy diagram of a three-level medium was shown in figure 1. The rate equations for the system are

$$\frac{dN_1}{dt} = -R_{13}N_1 + R_{31}N_3 - W_{12}N_1 + W_{21}N_2 + A_{21}N_2 \tag{41}$$

$$\frac{dN_2}{dt} = W_{12}N_1 - W_{21}N_2 + A_{32}N_3 \tag{42}$$

$$\frac{dN_3}{dt} = R_{13}N_1 - R_{31}N_3 - A_{32}N_3 \tag{43}$$

The pumping rates R_{13} and R_{31} are proportional to the pump intensity while the stimulated transition rates W_{12} and W_{21} are proportional to the combined signal and noise intensities. A_{21} and A_{32} are the spontaneous decay rates characteristic of the gain medium. The main difference between the simplified four-level and this three-level system is that these rate equations conserve the sum of the three population densities. Hence the total population density N_T is a constant (function of doping only) throughout the length of the amplifier.

$$N_T = N_1 + N_2 + N_3 \tag{44}$$

In steady state, the time derivatives are zero, hence from equations (41) and (42), N_1 and N_2 can

be solved in terms of N_T where

$$(R_{31} + R_{13} + W_{12})N_1 - (W_{21} + A_{21} - R_{13})N_2 = R_{31}N_T \tag{45}$$

$$-(W_{12} - A_{32})N_1 + (W_{21} + A_{21} + A_{32})N_2 = A_{32}N_T \tag{46}$$

and the solutions are

$$N_1 = \frac{\begin{vmatrix} R_{31} & -(W_{21} + A_{21} - R_{31}) \\ A_{32} & W_{21} + A_{21} + A_{32} \end{vmatrix}}{\begin{vmatrix} R_{31} + R_{13} + W_{12} & -(W_{21} + A_{21} - R_{31}) \\ -(W_{12} - A_{32}) & W_{21} + A_{21} + A_{32} \end{vmatrix}} N_T \tag{47}$$

$$N_2 = \frac{\begin{vmatrix} R_{31} + R_{13} + W_{12} & R_{31} \\ -(W_{12} - A_{32}) & A_{32} \end{vmatrix}}{\begin{vmatrix} R_{31} + R_{13} + W_{12} & -(W_{21} + A_{21} - R_{31}) \\ -(W_{12} - A_{32}) & W_{21} + A_{21} + A_{32} \end{vmatrix}} N_T \tag{48}$$

The denominators of N_1 and N_2 is

$$Det = (R_{31} + R_{13} + W_{12})(W_{21} + A_{21} + A_{32}) - (W_{21} + A_{21} - R_{31})(W_{12} - A_{32}) \tag{49}$$

33

In an ideal three-level medium, the transfer rate A_{32} is very fast compared with the stimulated transition rates hence in the limit,

$$Det \approx R_{31}A_{32} + (W_{12} + W_{21})A_{32} + A_{21}A_{32} \tag{50}$$

and consequently if $\dfrac{1}{\tau} = A_{21}$,

$$N_1 = \frac{W_{21}\tau + 1}{R_{31}\tau + (W_{12} + W_{21})\tau + 1} N_T \tag{51}$$

$$N_2 = \frac{R_{13}\tau + W_{12}\tau}{R_{31}\tau + (W_{12} + W_{21})\tau + 1} N_T \tag{52}$$

Note that the pump rate appears in both the numerator and denominator of N_2, and only in the denominator in N_1. This leads to a pump saturation effect in both the gain and noise performance of a three-level amplifier as shown later.

2. Gain and Noise Measure

For simplicity, the emission and absorption cross-sections are assumed to be symmetrical[12].

$$R_{13} = R_{31} = \gamma S_p; \quad W_{12} = W_{21} = \sigma_s S_+ \tag{53}$$

The gain coefficient thus becomes

$$\alpha = \frac{\sigma_s}{v_g}(N_2 - N_1) = \frac{\dfrac{\sigma_s}{v_g}(\gamma S_p \tau - 1) N_T}{1 + 2\sigma_s \tau S_+ + \gamma S_p \tau} \tag{54}$$

In addition to gain saturation by S_+ as in the case of a simplified four-level system, there is also saturation by pump power. This is the first pump saturation effect observed in the three-level system. This also leads to the expectation that the gain is probably not similar for forward and reverse pumped amplifiers (unlike four-level systems) since the pump distribution is different for different pumped amplifiers. Another characteristic of the three-level system is that there is a pump threshold of $\dfrac{1}{\gamma\tau}$ below which the medium becomes an absorber instead of an amplifier.

The second pump saturation effect is observed in the inversion factor χ

$$\chi = \frac{N_2}{N_2 - N_1} = \frac{\gamma S_p \tau + \sigma_s \tau S_+}{\gamma S_p \tau - 1} \tag{55}$$

where S_p appears both in the numerator and denominator. Again, the pump threshold is evident. In fact, the stronger the pump is, the better is the inversion parameter.

In analyzing a distributed amplifier such as a fiber amplifier, the signal and noise is cascaded from section to section. In another paper [14], Professor Haus (my thesis supervisor) showed that an amplifier cascade of amplifiers of different noise measures is optimized if the amplifier of lowest noise measure appears in front. The noise measure of a differential segment of amplifier is equal to $2g\chi$.

Thus in a distributed amplifier with varying pump intensity, the high pump levels must be at the amplifier input. This result predicts that a forward pumped three-level amplifier delivers better noise measure performance than a reverse pumped one since the pump is the greatest at the input of the amplifier. To compare this prediction with the analytical model developed here, computer simulations can be used to derive numerical solutions since analytical solutions are not possible. The equations that describe the forward and backward propagating photon numbers are

$$\frac{dS_+}{dx} = S_-$$
(56)

$$\frac{dS_-}{dx} = S_+ + 2g\chi = S_+ + 2g\frac{\gamma S_p \tau + 2\sigma_s \tau S_+}{\gamma S_p \tau - 1}$$
(57)

Forward and reverse pumping can be represented by

$$\frac{dS_p}{dz} = \mp \frac{\gamma}{v_g} S_p$$
(58)

36

where the $\mp$ signs hold for forward and reverse pumping respectively. Equation (58) can also be expressed in terms of the normalized length x

$$\frac{dS_p}{dx} = \pm \frac{\gamma}{\sigma_s} \frac{1 + 2\sigma_s \tau S_+ + \gamma S_p \tau}{(\gamma S_p \tau - 1)N_T} S_p \tag{59}$$

Simulation results of these analytical solutions support the predictions of cascading distributed amplifiers under forward and reverse pumping. Figure 7 illustrates the difference in signal, noise and pump distribution across the length of the amplifier for the two pump configurations (with equal input pump powers), while figures 8 and 9 show the differences in the inversion parameter χ and gain coefficient α. Noise performance is better for the forward pumped case, while gain performance is higher for the reverse pumped amplifier.
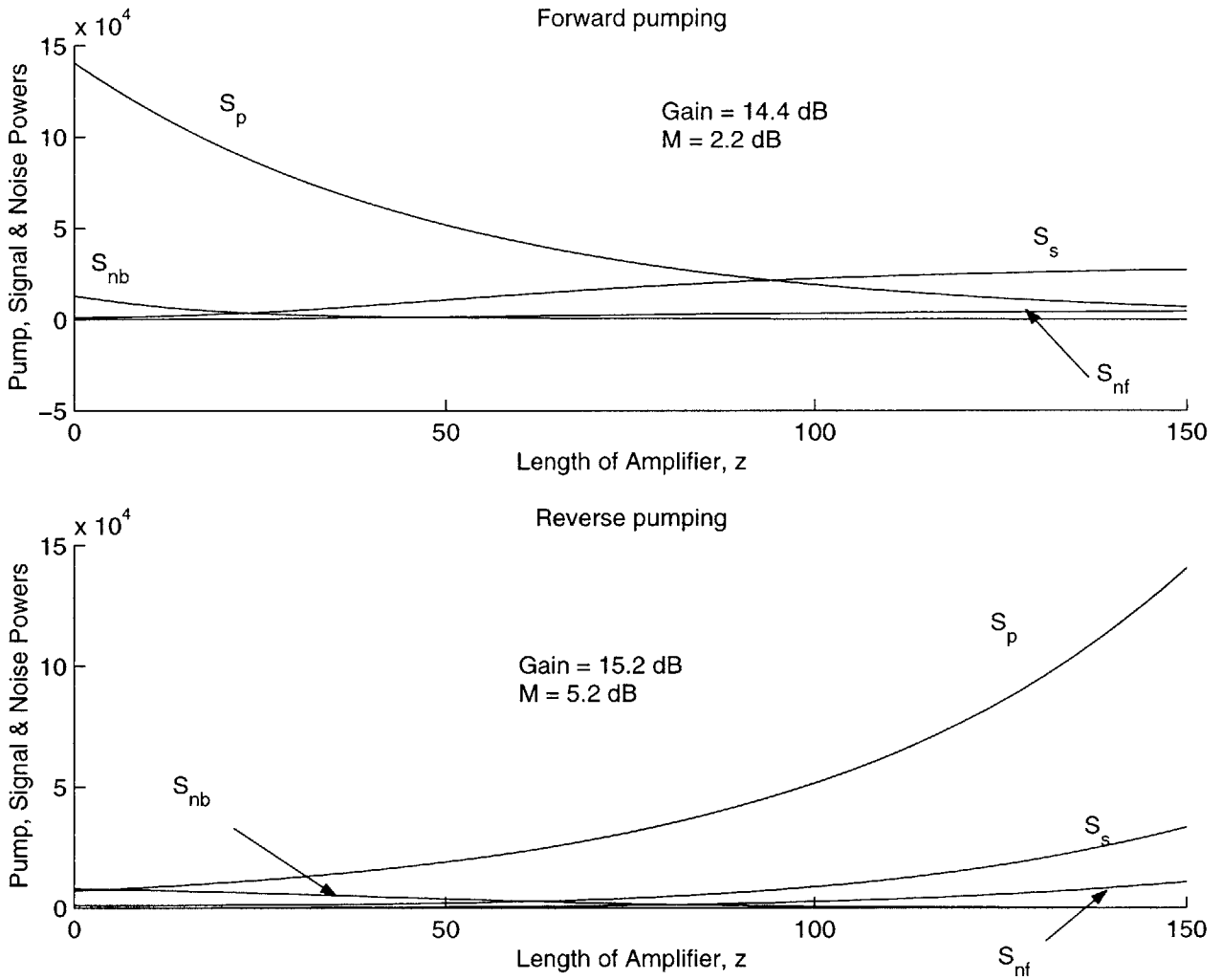
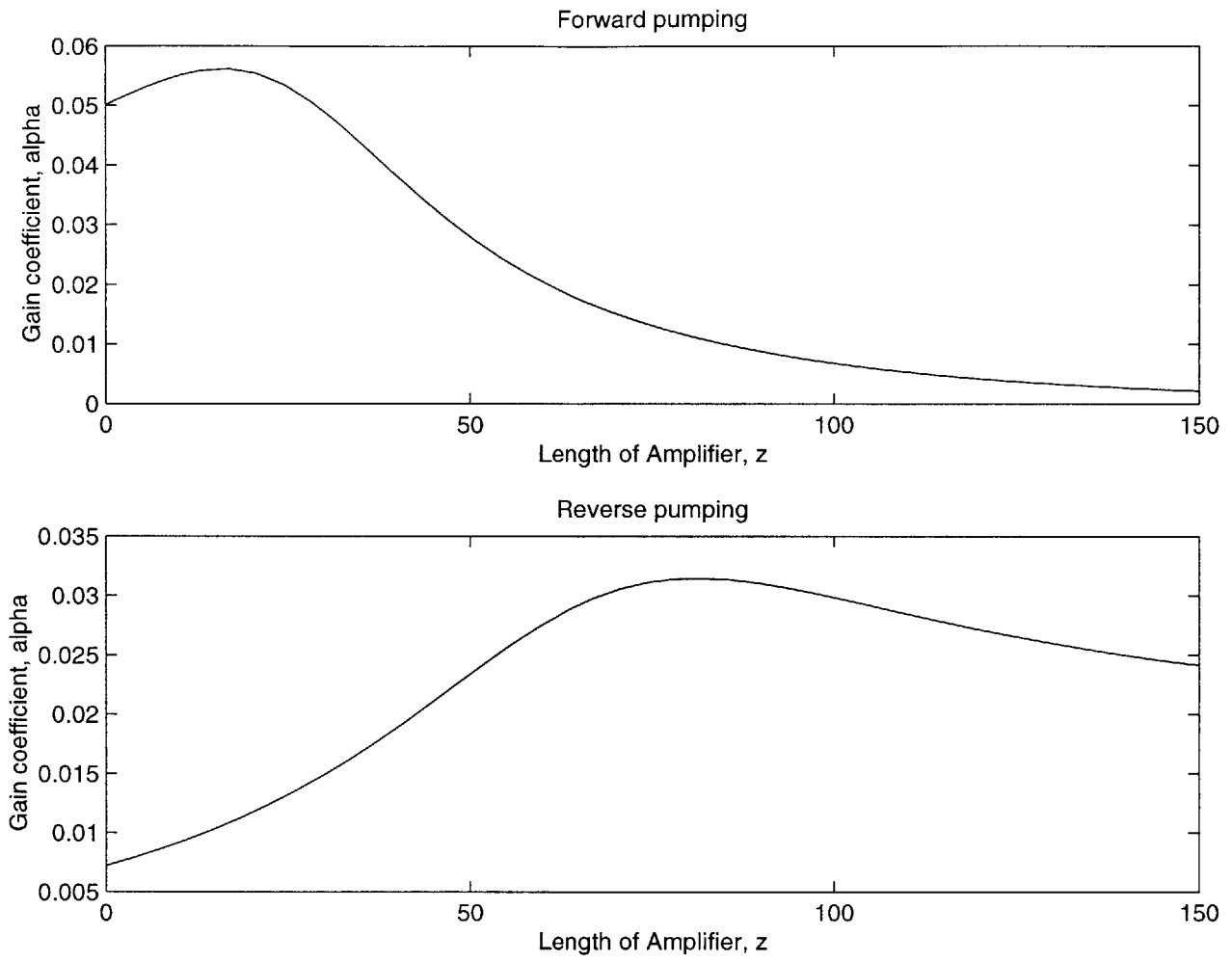Figure 7: Signal, noise and pump distribution for forward and reverse pumping

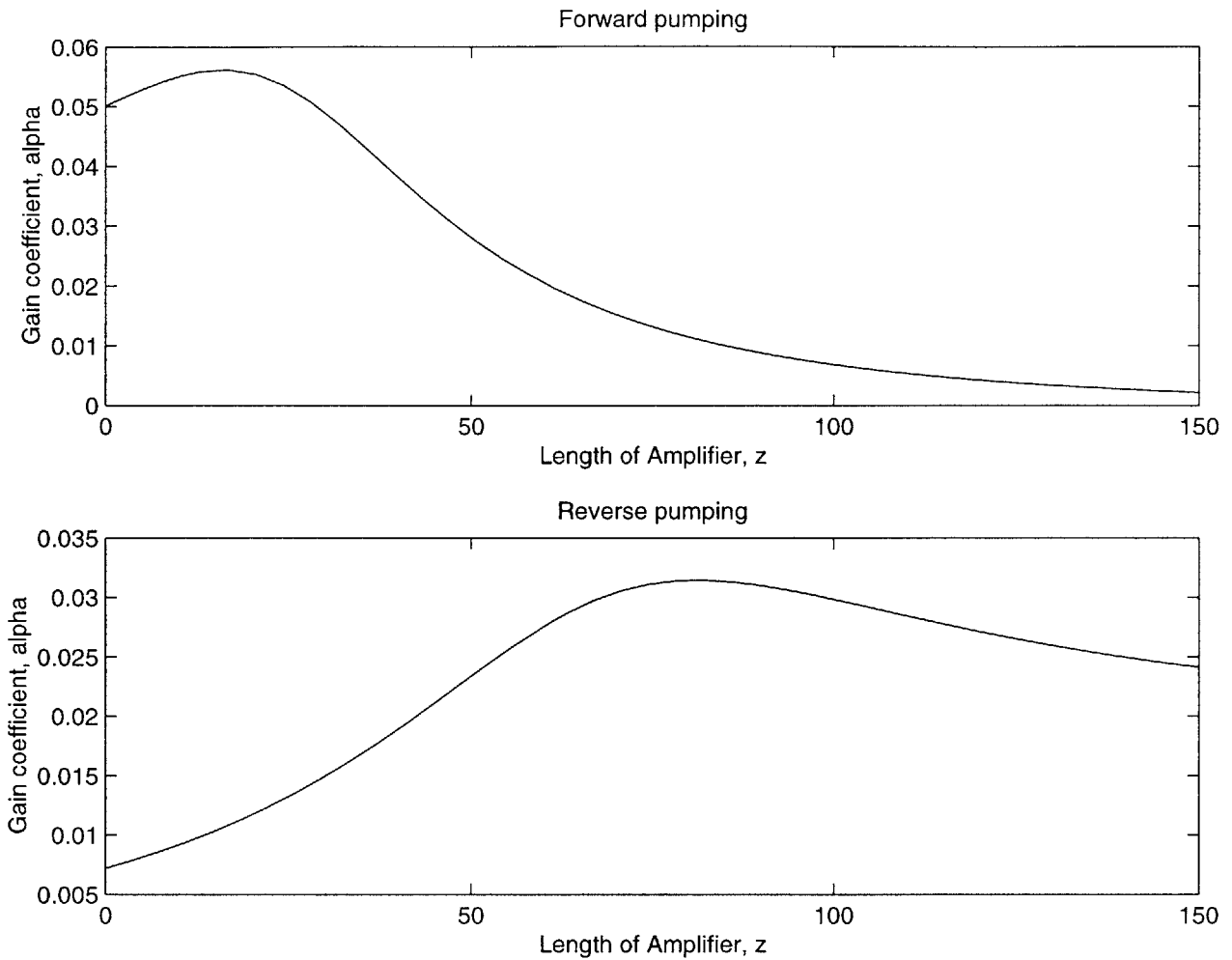Figure 8: Inversion parameter, χ for forward and reverse pumping

Figure 9: Gain coefficient, α for forward and reverse pumping

3. Middle Pumping

To test the validity of the predictions from forward and reverse pumping, another

computer simulation was conducted with the same length of amplifier and input pump power

except that the amplifier is now pumped from the middle instead of the beginning or end of the

amplifier[13]. This pump configuration should be expected to deliver better noise performance than

the reverse pumped amplifier, but slightly worse performance than the forward pumped one.

Furthermore, since the pump power is better utilized on both ends of the amplifier (especially for the first segment which is effectively backward pumped, hence achieves good gain), gain performance is expected to exceed both of the purely forward and reverse pumped configurations. The simulation results, shown in figures 10 and 11, support this argument. Table 2 summarizes the gain and noise performance for these three pump configurations.
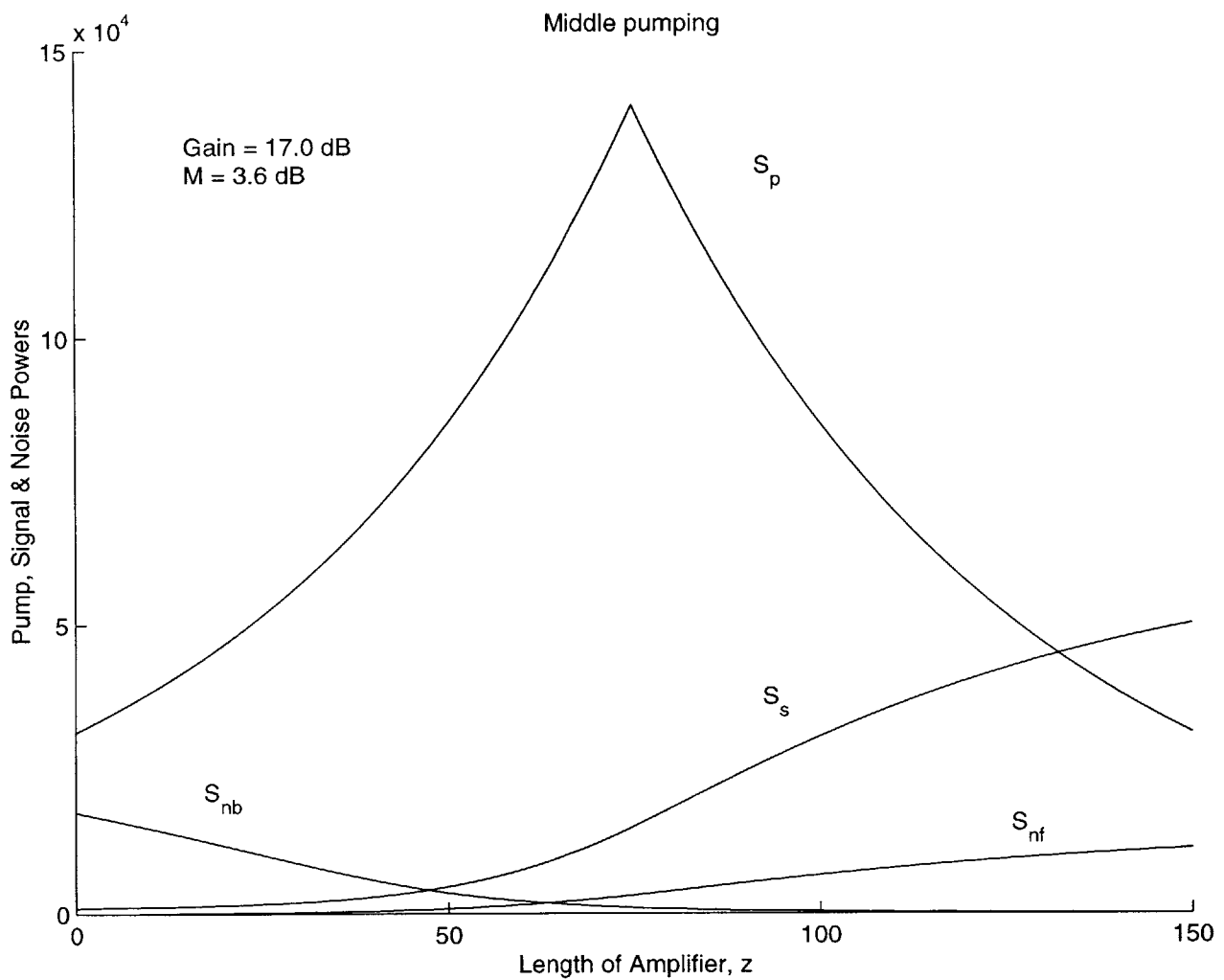

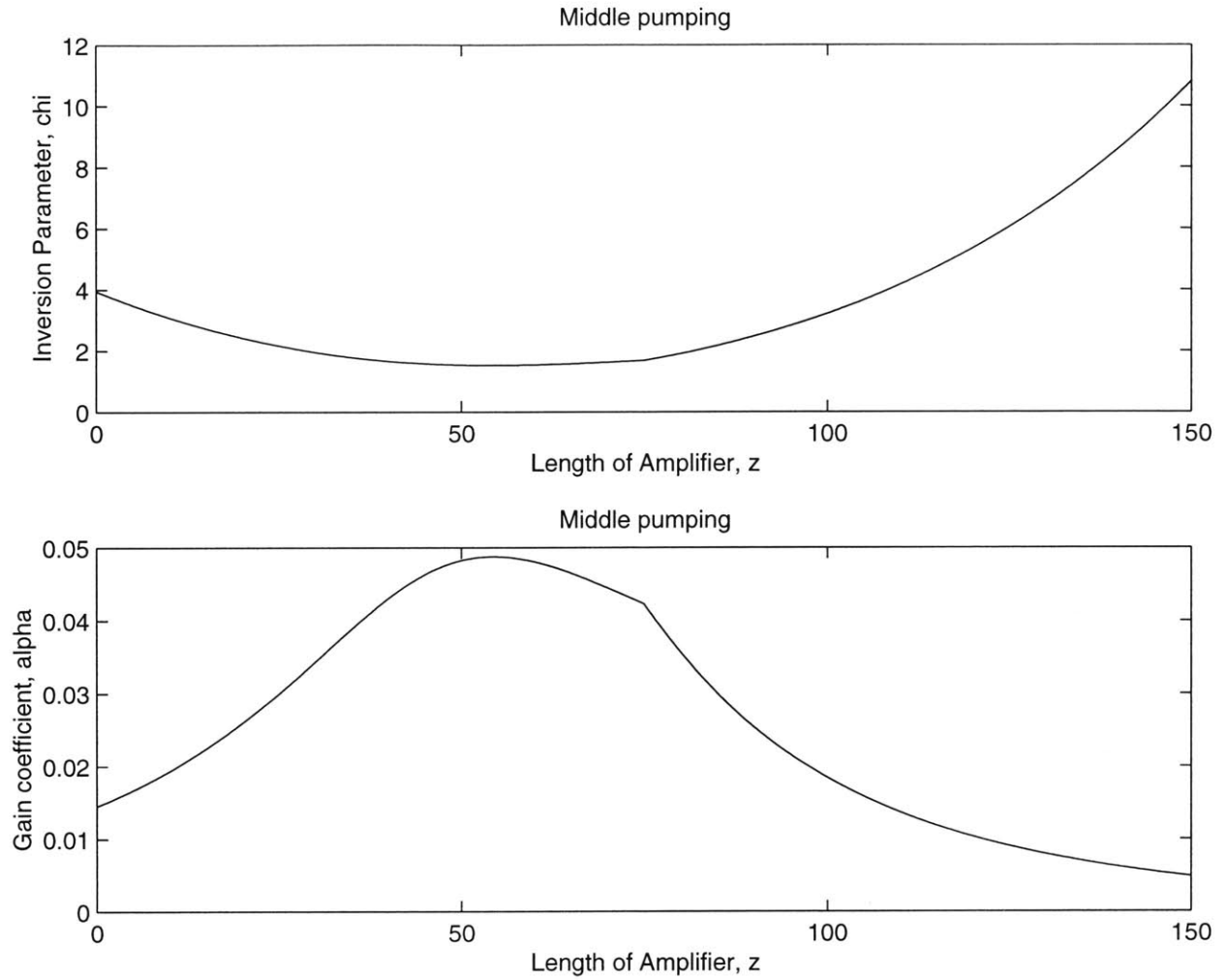Figure 10: Signal, noise and pump distribution for middle pumping

Figure 11: Inversion parameter, χ and gain coefficient, α for middle pumping

	Gain (dB)	M (dB)	Pump Efficiency (%)	SNR (dB)
Forward pumping	14.4	2.2	31.8	8.0
Reverse pumping	15.2	5.2	37.1	4.9
Middle pumping	17.0	3.6	56.2	6.5

Table 2: Summary table for the three pump configurations

V. Experimental Results & Analysis

A. Verifying the Four-Level Model

Most semiconductor lasers and almost all rare earth-doped fiber amplifiers for 1.3 μm signal wavelengths can be described as four-level systems[14]. Some of the most extensively studied examples in industry are the erbium-ytterbium (Er-Yb)-codoped amplifier, the neodymium (Nd)-doped and the praseodymium (Pr)-doped fiber amplifiers. However, these 1.3 μm amplifiers are not as commercially successful as the pure EDFA (which is a three-level system) because of their lower pump efficiency and more complex fiber processing techniques [2][15]. The advantage of these amplifiers over EDFAs is that in the event of a pump source failure, the former becomes transparent while EDFAs become a strong absorber of the signal because of a non-zero pump threshold [2].

As mentioned earlier, the predictions from the analytical four-level model have been verified experimentally for a forward and reverse pumped Er-Yb-codoped amplifier[16], a four-level system [1]. Thus I conclude that the theoretical model for the four-level system does describe real four-level amplifiers accurately.

B. Verifying the Three-Level Model

On the other hand, pure EDFAs are three-level systems [1,2] as shown in the energy level

43

structure in figure 2. For signal wavelengths of 1.5 μm, there are two pump wavelengths commonly used: $980\,nm$ and $1480\,nm$. I shall explain the differences between these two wavelengths later.

In the rest of this section, the theoretical model for the three-level system will be verified experimentally. First, the experimental setup chosen is explained. Then two experiments were carried out. The purpose of the first experiment is to verify the validity of the model description by fitting experimental results with simulations based on the analytical model. It is found that the three-level model does describe real EDFA amplifiers closely; hence the second experiment was conducted to compare the predictions from the simulations based on the theoretical model and experimental results. I will analyze the discrepancies between the analytical predictions and the experimental results, as well as explain some of the phenomena that were not predicted by the theoretical model. Modifications will then be made to the theoretical model to account for these newly observed trends.

C. Three-Level EDFA Experimental Setup

Two EDFA experiments were conducted to verify the predictions of the three-level analytical model introduced in this paper. The experimental setup is similar for both experiments and is shown in figure 12. The experiments were performed on a single erbium doped fiber segment at both 980 *nm* and 1480 *nm* pump wavelengths (of roughly the same input pump power)[17], and each under forward and reverse pumping.

The WDM coupler couples the pump wavelength to the signal wavelength before passing

the combined light into the amplifier. Forward and reverse pumping are achieved by putting the

WDM coupler either before or after the EDFA. The isolators prevent backward reflections.
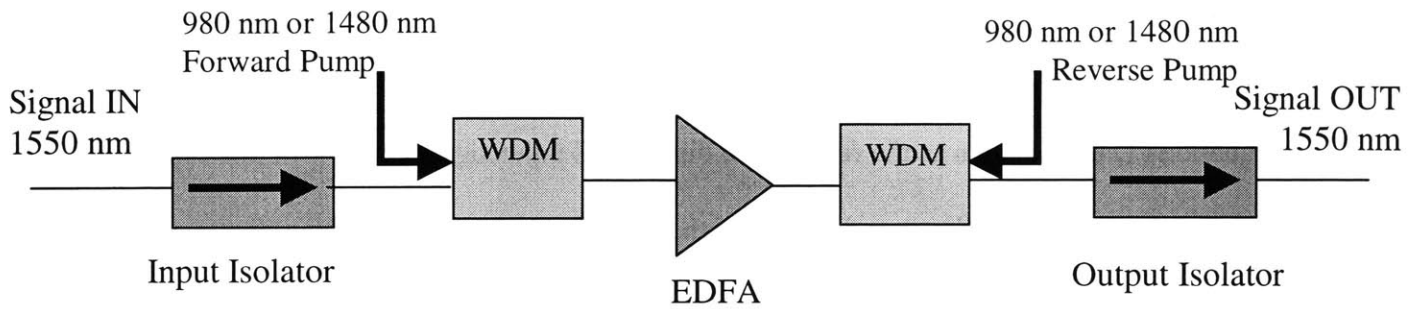
Estimated loss in coupler, filters and splices = 3.5 dB

Flters not shown in this diagram.[18]

WDM: Wavelength Division Multiplexer

Figure 12: Three-level EDFA experimental setup

D. Experiment 1: Verifying the Description of the Models

The first EDFA experiment was conducted for forward pumping at the 980 *nm*

wavelength and was carried out at Bell Laboratories, Lucent Technologies in the summer of

1999[19]. The purpose of this experiment is to verify that the theoretical three-level model describes

the EDFA. The gain and noise measure performance of the amplifier under different input signal

powers $S_{s,in}$ are used for comparison. Figures 13 and 14 show very good fits between

experimental data and simulation predictions, thus confirming the validity of the description of the

three-level model. Table 3 displays the values of the parameters used in the simulation.

g	γ	σ_s	β	N_t/v_g	L	$S_{p,in}$	τ
1.3	1	10	0.02	0.02	60	2.656e5	0.01

Table 3: Values of parameters used in simulation to fit data for experiment 1

Using the three-level theoretical model for forward pumping

Figure 13 illustrates the gain of the amplifier under increasing input signal power. Equation (1) defines gain as the ratio of the output and input signal powers. In this experiment, the signal powers at the input and output of the amplifier are measured with a power meter at the signal wavelength 1550 *nm*. The unit of measurement is *dBm*. In order to reduce the noise levels in the signal that would be detected by the power meter, the signal is first passed through a filter (not shown in figure 12). As $S_{s,in}$ increases, the gain decreases since the amplifier saturates given a limited pump power. A high level of saturation occurs when almost all the inverted population at the metastable level has been emitted through stimulation by the signal, thus producing very poor inversion levels with increasing $S_{s,in}$.
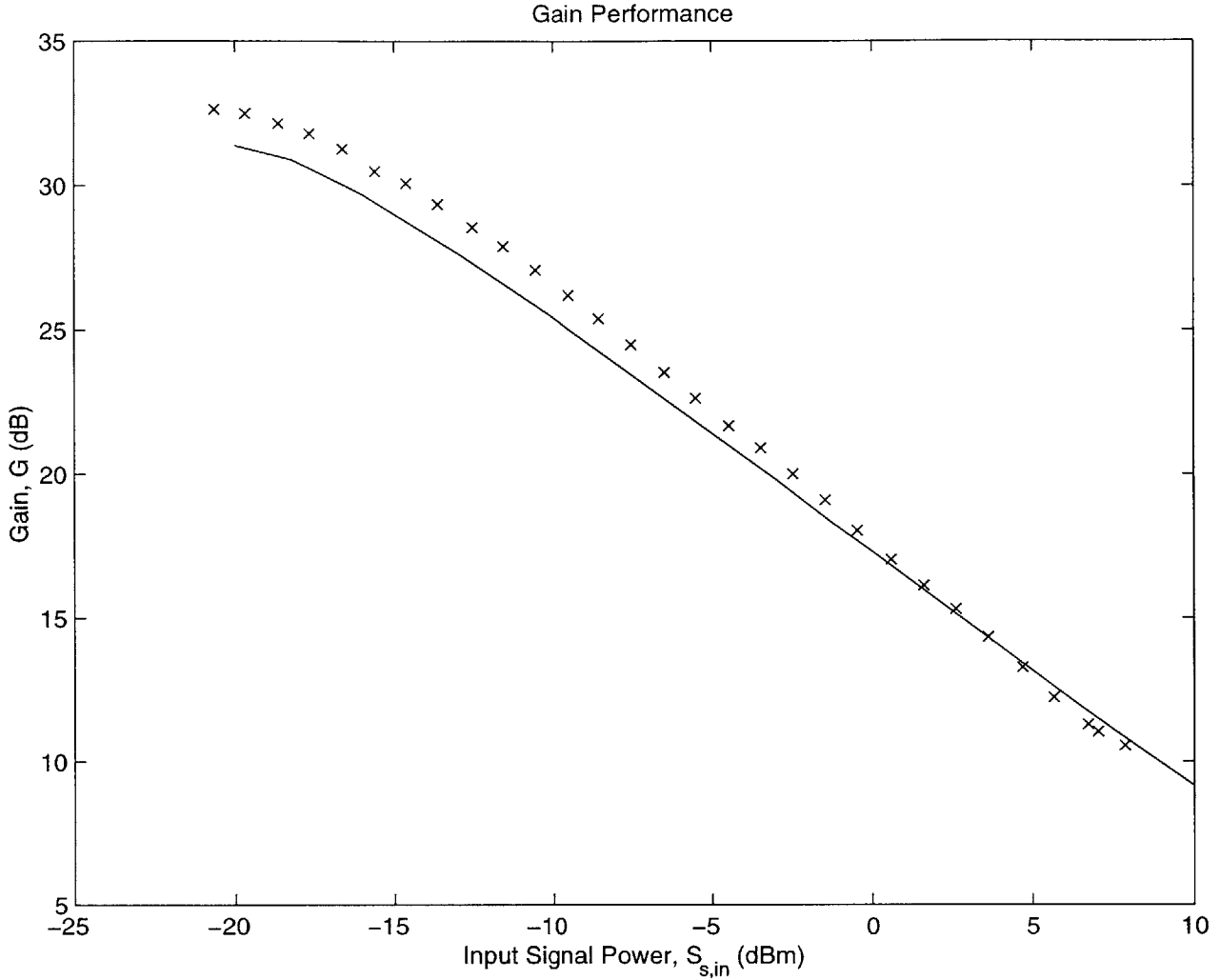
Figure 13: Gain measurements for experiment 1 (with simulation predictions)

Figure 14 shows the noise figure measurements for the same amplifier under the varying

$S_{s,in}$. An optical spectrum analyzer was used (not shown in the experimental setup in figure 12) to

measure the optical SNR at the output of the amplifier. From the optical output SNR and output

signal power, ASE power at the amplifier output was obtained. This result was then converted to

an equivalent ASE photon number $< n_{ASE} >$ within the signal bandwidth by division of the signal

filter bandwidth (in this experiment, filter bandwidth was 0.1 nm) [17]. F was then calculated

according to equation (3). It is a well-proven fact [1] that equation (3) can be reduced to

$$F \approx \frac{1}{G} + 2n_{sp}(1 - \frac{1}{G}) \tag{60}$$

where n_{sp} is the spontaneous emission enhancement factor and is equivalent to the inversion

parameter, χ used in computing the noise measure of the theoretical models. In the limit of large

G, equation (60) further reduces to

$$F \approx 2n_{sp} \tag{61}$$

Thus in the limit of large G, the noise measure M used in the theoretical model is related to the

noise figure definition F used in industry according to

$$F \approx 2M \tag{62}$$

This straightforward relationship between F and M, equation (62), thus allows noise

measurements from the experiments and simulations to be easily compared as shown in figure 14.

Figure 14 shows noise figure measurements with varying input signal power. As

$S_{s,in}$ increases initially, noise figure is reduced corresponding to an improving noise performance.

This is because at a particular saturation level, a stronger signal means that less noise is present.

However, as the amplifier saturates with too much input signal power, the inversion becomes

worse. Therefore noise figure starts to increase with amplifier saturation.
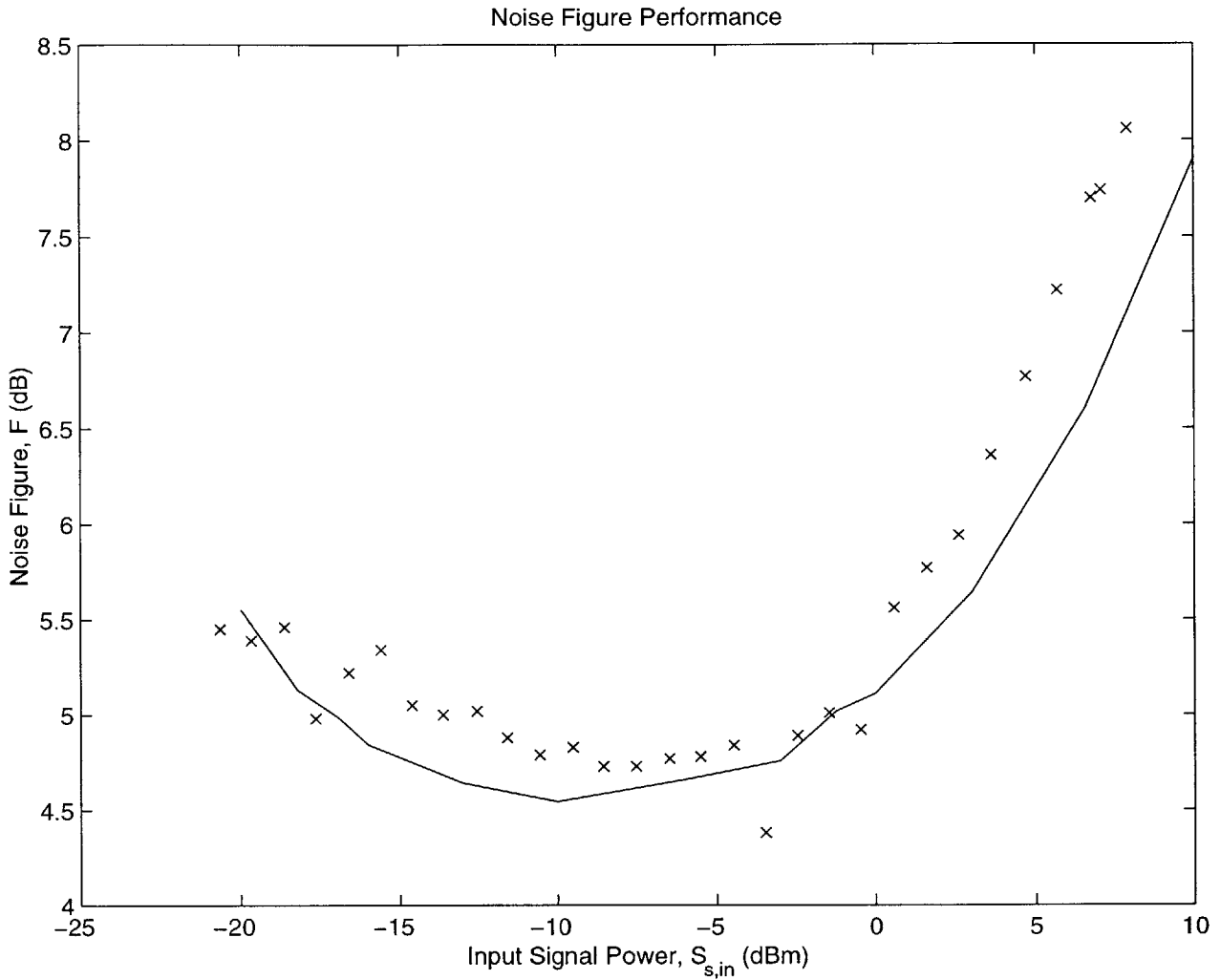
Figure 14: Noise figure measurements for experiment 1 (with simulation predictions)

E. Experiment 2: Comparing 980 nm and 1480 nm Pumping

Having shown with the first experiment that the theoretical three-level model does

describe EDFA behavior accurately, a second experiment was carried out to test the predictions

from the model. This experiment was conducted in MIT[20]. Figures 15 and 16 show the

experimental results for forward and reverse pumping at both wavelengths. The same

experimental setup is used for both wavelengths except that the filter bandwidth used for 980 *nm*

pumping is about 0.1 *nm* while that used for 1480 *nm* pumping is about 0.5 *nm*.

From these figures, I first verify that the amplifier under forward pumping delivers better

noise performance than that under reverse pumping, at both pump wavelengths. Gain performance

is also higher under reverse pumping at both wavelengths. These observations are consistent with
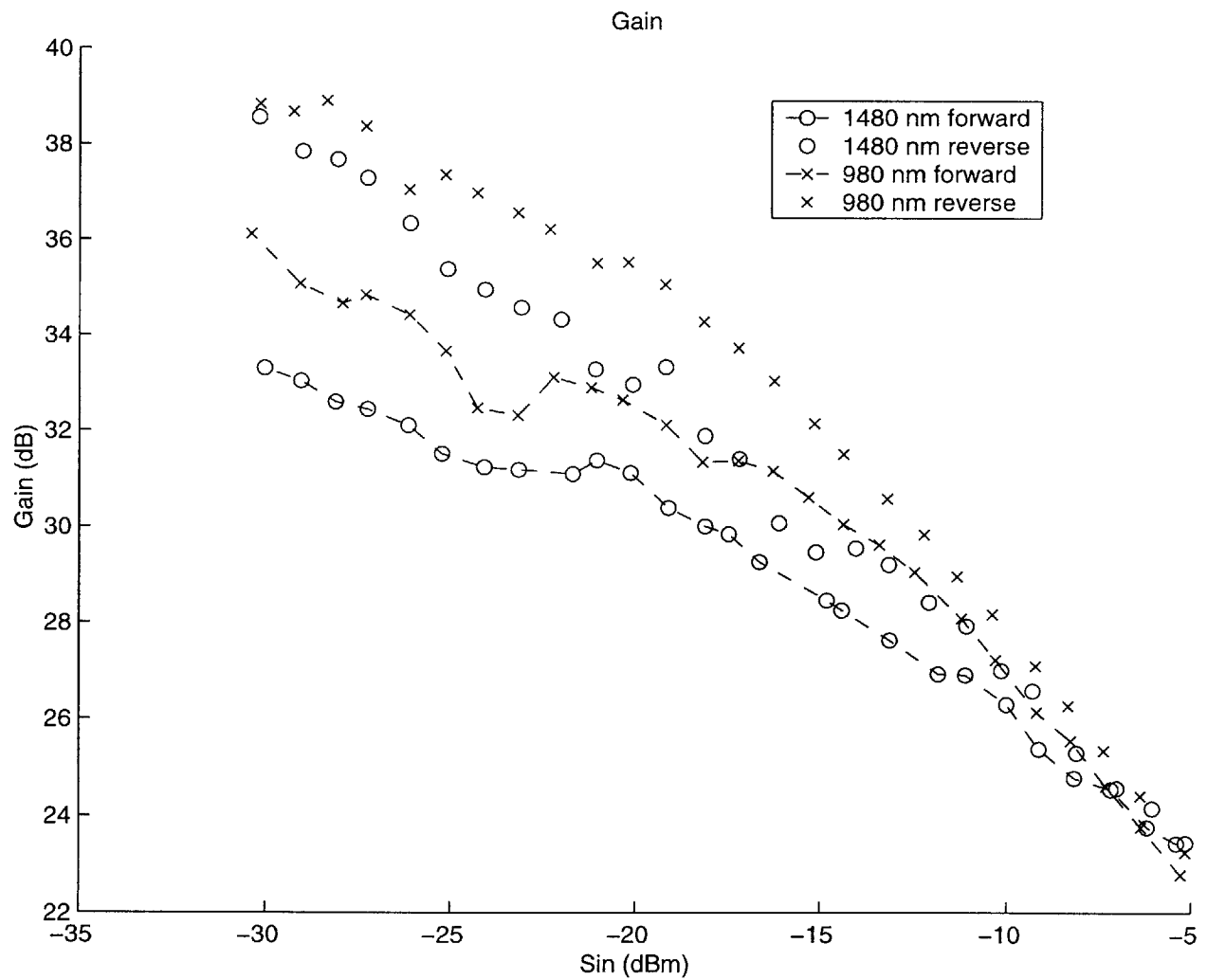
the predictions from the theoretical model.

Figure 15: Gain measurements for experiment 2

Noise Figure

20

18

16

Noise Figure (dB)

14

12

10

8

6

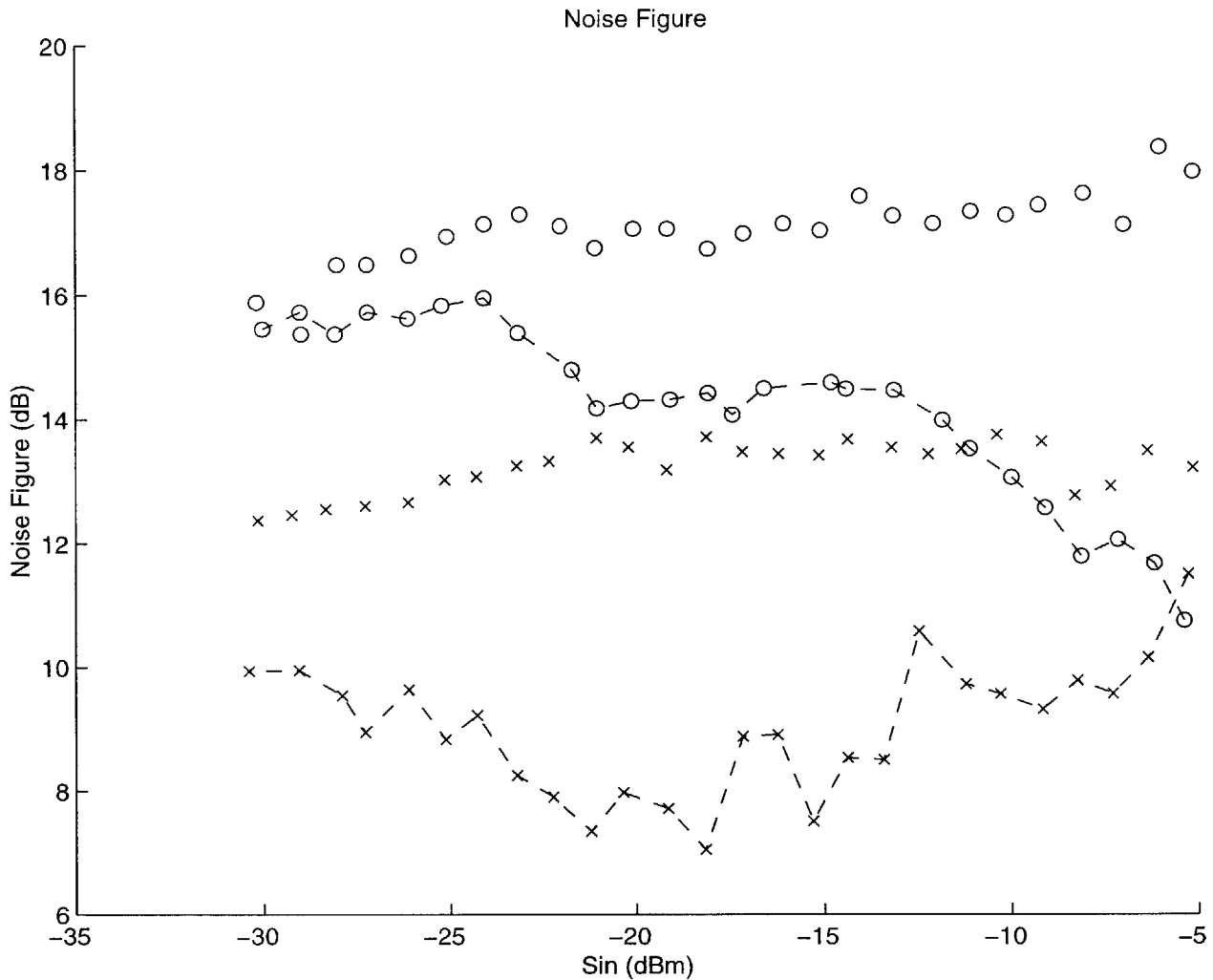-35   -30   -25   -20   -15   -10   -5

Sin (dBm)

Figure 16: Noise figure measurements for experiment 2

An interesting second observation from figure 16 is that noise figure is higher at the 1480

nm wavelength than at 980 *nm* for all input signal powers. This can be explained by modifying the

three-level analytical model introduced in the earlier section. [2] argues that the assumption of

pump relaxation rate A_{32} being very fast compared to the other transition cross-sections is only

valid for certain pump wavelengths, 980 *nm* being one of them. In other pump configurations,

such as the 1480 *nm* one, the excited pump level is almost identical to the metastable level (1480

nm pump and 1550 *nm* signal) so they belong to the same multiplet as illustrated in figure 17

(adapted from [2]). In this case, the population at the pump level is not zero but consists of some

finite thermal population since there will be thermal equilibrium within a given multiplet (assuming

that the thermal equilibration time is very short compared to the overall multiplet decay rates to

lower levels). Hence, there will be stimulated emission at the pump frequency as well as the signal

frequency. This explains why the quantum efficiency is lower for 1480 *nm* than 980 *nm*.

The 980 *nm* pump wavelength thus yields higher gains than a 1480 *nm* pump at high

powers because it achieves higher population inversion or has higher quantum efficiency [2].

Because of the higher inversion of a 980 *nm* -pumped amplifier, its noise measure is also better
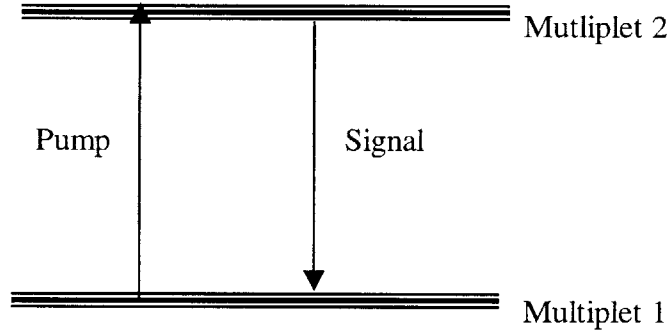
than a 1480 *nm* amplifier.

Figure 17: Energy level of a two-multiplet system [2]

Thus a non-ideal three-level system, A_{32} is not infinite, and equations (47) and (48)

become

$$N_1 = \frac{R_{31}W_{21} + R_{31}A_{21} + W_{21}A_{32} + A_{21}A_{32}}{Det} N_T \qquad (63)$$

$$N_2 = \frac{R_{13}A_{32} + W_{12}A_{32} + R_{31}W_{12}}{Det} N_T \tag{64}$$

where *Det* is as defined in equation (49). Together with equation (53) and $\frac{1}{\tau} = A_{21}$, the inversion

parameter becomes

$$\chi = \frac{(\gamma S_p \tau + \sigma_s \tau S_+)A_{32} + \gamma S_p \sigma_s S_+ \tau}{(\gamma S_p \tau - 1)A_{32} - \gamma S_p \tau} \tag{65}$$

By replacing $\tau_{21} = \tau = \frac{1}{A_{21}}$ and $\tau_{32} = \frac{1}{A_{32}}$ in equation (65), it can be shown that for a 1480 nm

pumped amplifier,

$$\chi = \frac{\gamma S_p \tau_{21} + \sigma_s S_+ \tau_{21} + \gamma S_p \sigma_s S_+ \tau_{21} \tau_{32}}{\gamma S_p \tau_{21}(1 - \tau_{32}) - \gamma S_p \tau_{21} \tau_{32} - 1} \tag{66}$$

$$\alpha = \frac{\sigma_s}{\nu_g} \frac{\gamma S_p(\tau_{21} - \tau_{32}) - 1}{1 + 2\sigma_s S_+ \tau_{21} + \gamma S_p(2\tau_{32} + \tau_{21}) + 3\gamma S_p \sigma_s S_+ \tau_{21} \tau_{32}} N_T \tag{67}$$

which are reduced to equations (55) and (54) respectively as $\tau_{32} \to 0$ for the 980 nm pumped

model. Comparing equation (65) with equation (55), the added terms are $\gamma S_p \sigma_s S_+ \tau$ in the

numerator and $-\gamma S_p \tau$ in the denominator; hence noise performance is definitely worse for the

1480 *nm* than the 980 *nm*, which is consistent with the experimental results shown in figure 16.

To test the predictions from the theoretical three-level model for 980 *nm* and the modified model for 1480 *nm*, the experimental data shown in figures 15 and 16 are fitted with simulations from the models. Figures 18 and 19 verified the predictions from the simulations fit the experimental data quite well at both wavelengths, given measurement errors of the OSA. Tables 4 and 5 show the values of the parameters used in the corresponding simulations to fit the data at each wavelength.

g	γ	σ_s	β	N_t/v_g	L	$S_{p,in}$	τ
2	0.005	20	0.02	0.02	300	8.069e9	0.01

Table 4: Values of parameters used in simulation to fit data for experiment 2 at 980 *nm*
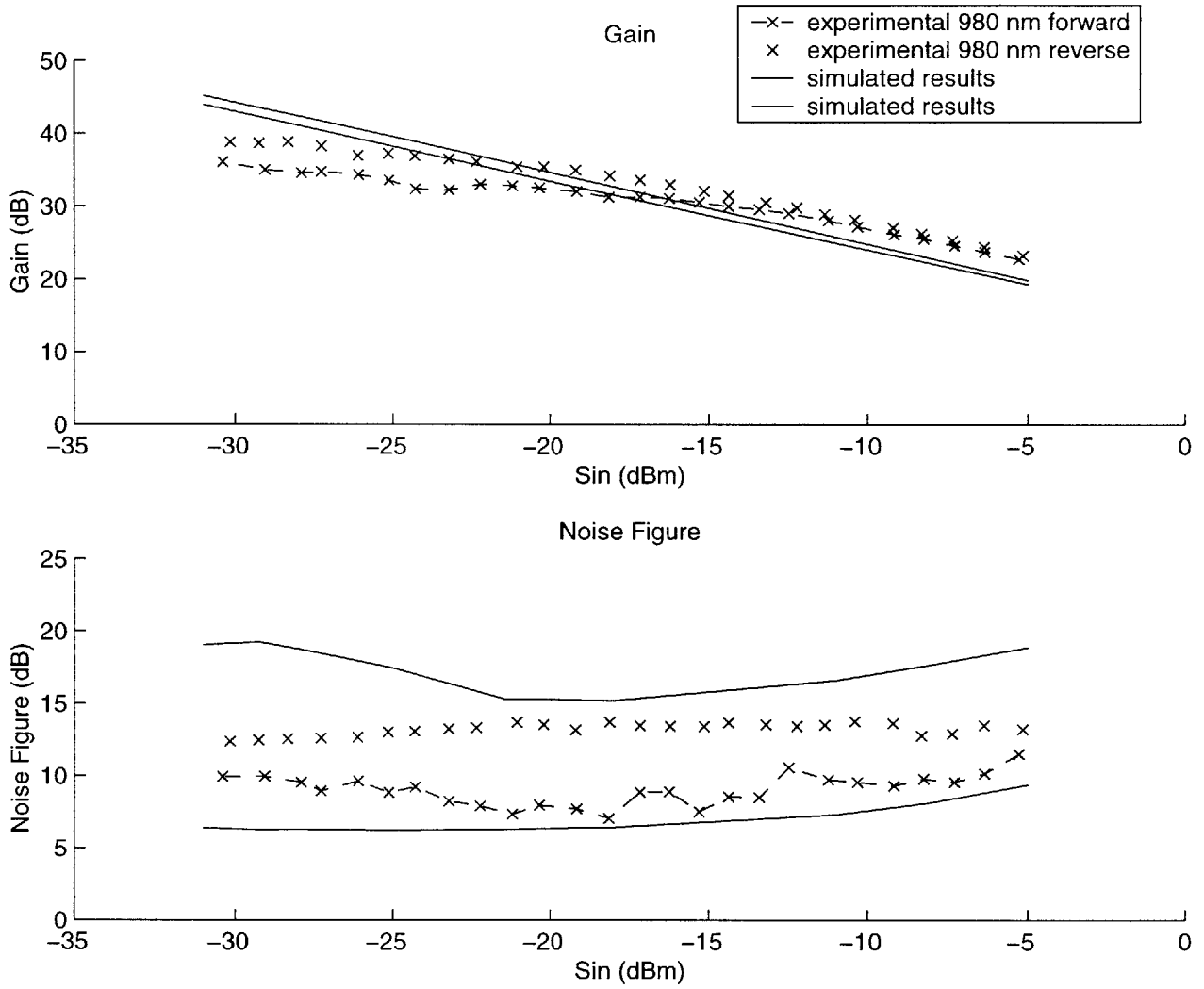*Using the three-level theoretical model for 980 nm*

Figure 18: Comparison between simulation and experimental data at 980 *nm*

g	γ	σ_s	β	N_t/v_g	L	$S_{p,in}$	τ_{21}	τ_{32}
2	0.005	50	0.02	0.02	300	8.069e9	1e-4	1e-7

Table 5: Values of parameters used in simulation to fit data for experiment 2 at 1480 *nm*

Using same amplifier length and input pump power as Table 4

but different amplifier characteristics because of modified 1480 nm model
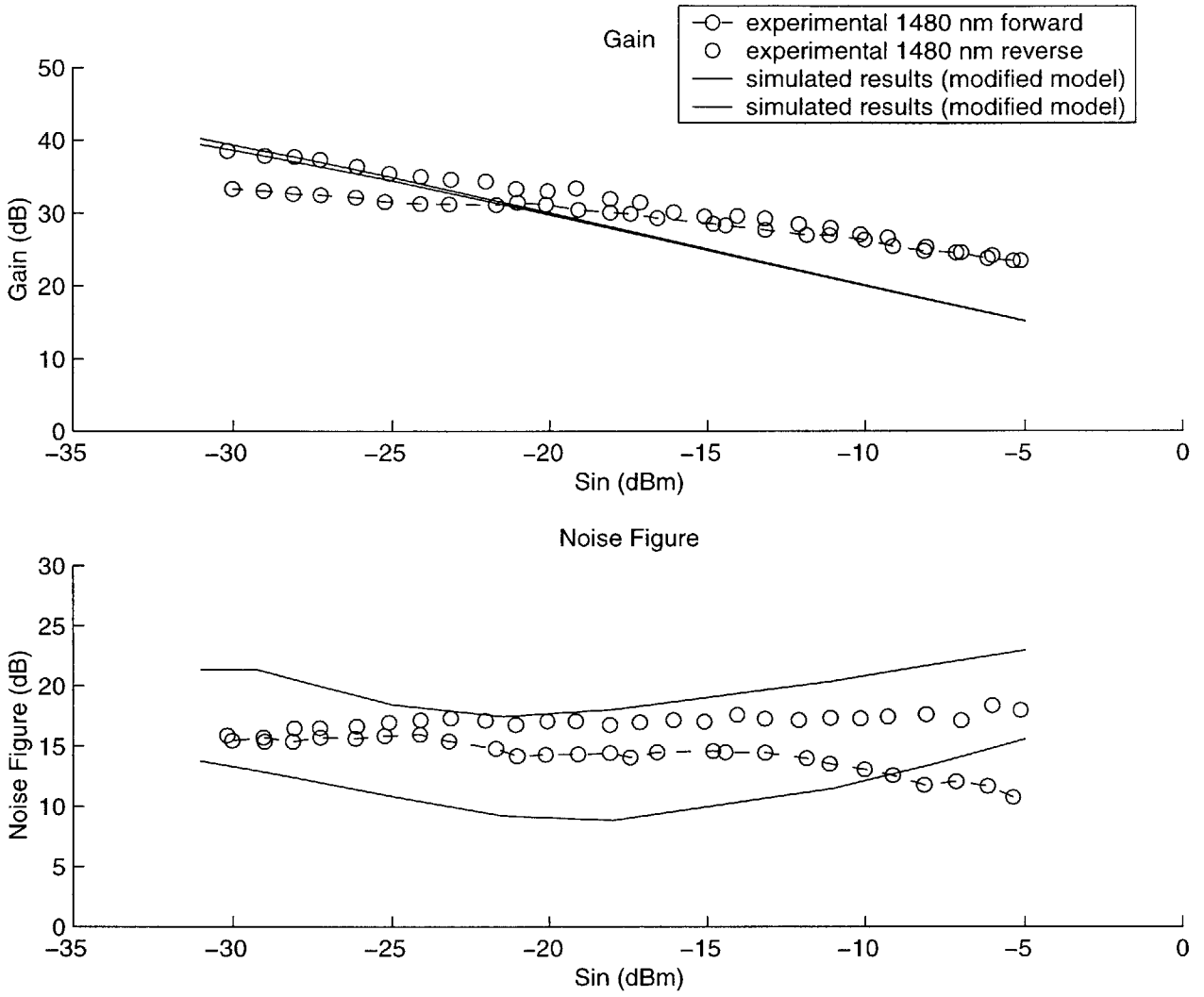
Figure 19: Comparison between simulation and experimental data at 1480 *nm*

VI. Conclusions

Optical amplifiers can be described as four-level or three-level media. Their noise optimization is quite different. In the simplified four-level model, closed-form analytical results were obtained which were previously not known to the industry. It was found analytically that the inversion parameter is independent of the pump which leads directly to the conclusion that there is no difference between the noise performance for forward and reverse pumping of the amplifier. The symmetrical behavior between forward and reverse pumping is in direct contradiction to the behavior of most practical optical amplifiers. The discrepancy arises because most practical optical amplifiers are more aptly described as three-level systems. However, recent experimental work shows that co-doped Er-Yb amplifiers do display this symmetrical behavior and [1] suggests that these amplifiers display better gain performance than EDFA but lower pump efficiencies because of a shorter lifetime of the metastable state. Thus there is potential to improve the pump efficiency of four-level amplifiers for more extensive practical use. My theoretical work in this paper hence provides the framework for further research on these four-level amplifiers.

On the other hand, for a three-level medium, the pump does appear in the inversion parameter and the stronger the pump, the better the inversion. Since the noise measure of an amplifier segment is a function only of the inversion parameter, and the noise measure defines the noise performance of the amplifier, it is a simple rule to place the amplifier segment with the lowest noise measure, and thus with the highest pump level, at the amplifier input. Therefore, three-level amplifiers achieve the best noise performance under forward pumping, albeit at the

expense of gain. The three-level theoretical model thus verifies the result observed in most

practical amplifiers, a result that was never explained analytically before. In contrast to most

numerical models of these amplifiers used in industry today, the simple analytical approach used in

this paper provides a more intuitive understanding of the physical mechanisms at work. Besides,

the model is quite easily extendable as shown in the modification made in the model to

differentiate between the 980 *nm* and 1480 *nm* pumping.

VII. Bibliography

[1] E. Desurvire, *Erbium-Doped Fiber Amplifiers; Principles and Applications*, New York: John Wiley and Sons, 1994.

[2] P.C. Becker, N.A. Olsson, J.R. Simpson, *Erbium-Doped Fiber Amplifiers – Fundamentals and Technology*, Academic Press, 1999.

[3] Ivan P. Kaminow and Thomas L. Koch, *Optical Fiber Telecommunications III A, B*, Lucent Technologies, 1997.

[4] S. Shimada and H. Ishio, *Optical Amplifiers and their applications*, John Wiley and Sons, 1994.

[5] Michael J.F. Digonnet, *Rare Earth Doped Fiber Lasers and Amplifiers*, Marcel Dekker, Inc., 1993.

[6] H. A. Haus, "An Extension of the Noise Figure Definition," IRE Proc. **45** (1957).

[7] H. A. Haus, Subcommittee 7.9 on Noise, Chairman, "IRE Standards on Methods of Measuring Noise in Linear Twoports, 1959," Proc. IRE **48**, 60-74 (1960).

[8] H. A. Haus, "Noise Figure Definition Valid from RF to Optical Frequencies," CHAOS, accepted for publication.

[9] H. A. Haus and R. B. Adler, "Optimum Noise Performance of Linear Amplifiers," Proc. IRE **46**, 1517-1532, 1958.

[10] H. A. Haus and R. B. Adler, "Canonical Form of Linear Noisy Networks," IRE trans. Circuit Theory **CT-5**, 161-167, 1958.

[11] H. A. Haus, "The Proper Definition of Definition of Noise figure of Optical Amplifiers," Optical Fiber Communication Conference, 1999.

[12] H. A. Haus and R. B. Adler, "Network realization of optimum amplifier noise performance," IRE Trans Cir. Theory **CT-5**, 156-161, September 1958.

[13] H. A. Haus and R. B. Adler, *Circuit Theory of Linear Noisy Networks*, MIT Press, Cambridge MA 1959.

[14] H.A. Haus, Invited paper.

[15] M. Movassaghi, M. K. Jackson, V. M. Smith, and W. J. Hallam, "Noise Figure of Erbium-Doped Fiber Amplifiers in Saturated Operation," Journal of Lightwave Technology **Vol 18 No. 3**, May 1998.

[15] B. E. A. Saleh and M.C. Teich, *Fundamentals of Photonics*, John Wiley and Sons, 1991.

[16] A. E. Siegman, *Lasers*, University Science Books, 1986.

[17] Dennis Derickson, *Fiber Optic Test & Measurement*, by Prentice Hall, 1998.

---

[1] I would like to point out that in addition to my approach in this paper, an alternative is the use of forward-error-correction (FEC) in the encoding/decoding of the signals. With FEC, higher errors can be tolerated in the transmission fiber without compromise of information integrity because the receiver at the other end of the transmission channel can always recover from those errors by decoding. However, this approach is not being pursued in this paper.

[2] Erbium (Er) is trivalent and has atomic number 68 in the periodic table. It is a rare earth element, and in particular belongs to the family of lanthanides. (Rare earth elements are divided into lanthanides and actinides.)

[3] The lifetime of a level is inversely proportional to the probability per unit time of the relaxation of an atom from that excited level to a lower energy level.

[4] Cross-sections quantify the ability of an ion or atom to absorb and emit light. They are related to the Einstein A and B coefficients. The cross section of the transition between the $^4I_{13/2}$ and $^4I_{15/2}$ states represents the probability for that transition to occur with the concurrent emission or absorption of light.

[5] The transition probability for the absorption of a photon of the corresponding energy gap is proportional

to cross section and the intensity of the incident light.

[6] A low pump threshold means that less pump photons are needed per unit time to maintain the inversion level.

[7] Another caution of using a long amplifier is that lasing might occur where unwanted backward reflections get amplify in the lasing medium and produce lasing at an unwanted frequency other than the signal frequency.

[8] Refer to [1-5] for the general properties of optical amplifiers, in particular EDFAs.

[9] This model has been developed by Professor H.A. Haus and me. It has also been previously reported in an internal memo Quantum Electronics and Femtosecond Optics Memo No. 94, "Noise Figure of Forward and Reverse Pumped Fiber Amplifiers".

[10] This work was presented by J.-M. P. Delavaux, C. McIntosh, J. Shmulovich, A.J. Bruce, R.K. Pattnaik and B.R. Wirstiuk from Lucent Technologies, Bell Laboratories and Lehigh University, Physics Department. The title of the talk was "Gain Flatness of a Planar Optical Waveguide Amplifier (POWA)" and was presented at the Optical Fiber Conference (OFC) 2000.

[11] Refer to endnote 10.

[12] Actually, the emission and absorption cross-sections are only equal if the transition states are both degenerate. Experimental studies have shown that this is a fair assumption to make in most rare earth-doped fiber amplifiers. [2] show a more rigorous treatment of the asymmetry between the emission and absorption cross-sections using the standard Einstein theory and McCumber treatment.

[13] These simulations do not take into account the losses associated with the couplers or connectors, i.e. assumed to be in perfect operating conditions. However, these losses are not significant given the technology available today; typically, a WDM (Wavelength Division Multiplexer) coupler to couple the signal and pump together achieves as little as 0.3 dB loss.

[14] To see the energy level structures of Nd- and Pr-doped fibers, please refer to [5] pp 243 Figure 2 (Nd-doped), and [2] pp 405 Figure 10.3 (Pr-doped).

[15] From [2], The lower pump efficiency of these 1.3 μm amplifiers necessitates higher pump levels than their erbium cousins. Another factor in favor if EDFA is that these 1.3 μm amplifiers require fluoride fiber processing and fabrication technology which is less widespread and more complex than that of silica fibers required by EDFAs.

[16] Refer to endnote 10.

[17] Actually, the input pump power was higher for the 980 nm-pumped amplifier than the 1480 nm-pumped one. Hence, the output saturation power is the same for both amplifiers despite the 1480 nm-pumped amplifier known for having a higher gain typically [3].

[18] Filters are not shown in this diagram. There is an input and output filter attached to the input and output

of the amplifier respectively before measuring the signal input and output power (so as to exclude the noise power).